THE SYNTHESIS AND DEVELOPMENT OF F-18 LABELING SUBSTRATES FOR *IN VIVO* PET IMAGING STUDIES

by

Katarina Rohlfing

A thesis submitted to the Faculty of the University of Delaware in partial fulfillment of the requirements for the degree of Master of Science in Chemistry and Biochemistry

Fall 2016

ProQuest LLC.
789 East Eisenhower Parkway
P.O. Box 1346
Ann Arbor, MI 48106 – 1346

THE SYNTHESIS AND DEVELOPMENT OF F-18

LABELING SUBSTRATES FOR *IN VIVO*

PET IMAGING STUDIES

by

Katarina Rohlfing

Approved: _____

Joseph M. Fox, Ph.D.
Professor in charge of thesis on behalf of the Advisory Committee

Approved: _____

Murray V. Johnston, Ph.D.
Chair of the Department of Chemistry and Biochemistry

Approved: _____

George H. Watson, Ph.D.
Dean of the College of Arts and Sciences

Approved: _____

Ann L. Ardis, Ph.D.
Senior Vice Provost for Graduate and Professional Education

ACKNOWLEDGMENTS

I would first like to thank my network of family and friends for their continued love and support over the years. They have provided me with strength and encouragement during my academic studies as well other endeavors throughout my life. I am extremely grateful for all of their advice and guidance.

To my advisor Joe, you have not only been an amazing research advisor, but a mentor as well. I could never thank you enough for your support during my graduate studies and for helping to guide me on the right path towards success. I am tremendously appreciative of the experience I have received while working in your lab and the skills I have acquired working on the projects you have assigned to me. I owe you a debt of gratitude.

I would also like to thank the Fox group members. I am honored to have been surrounded by so many talented chemists with inviting personalities. You have all given me suggestions when I have asked for help and have made my experience that much more enjoyable. A special thank you goes to Samuel Scinto for all of your help with my one of my projects and biochemistry skills you have taught me.

Finally, I would like to thank the administrative staff and chemistry and biochemistry faculty at the university. You have all been extremely supportive in my academic studies when I have needed help. A special thank you also goes to Dr. Thorpe for your all of your advice and suggestions on one of my research projects.

TABLE OF CONTENTS

LIST OF TABLES

LIST OF FIGURES

LIST OF SCHEMES

ABSTRACT

The rapid bioorthogonal reaction between tetrazines and *trans*-cyclooctenes has been used for a number of scientific applications, one of which includes the rapid assembly of F-18 probes for PET imaging. Due to the fast reactivity between these substrates and efficiency at low concentrations, the tetrazine ligation makes it an unusually well-suited reaction for radiolabeling applications.

Discussed in Chapter 1 is the development of a second generation ^{18}F-labeling system based on a conformationally strained *trans*-cyclooctene (sTCO). This dienophile, which is two orders of magnitude more reactive than conventional TCO derivatives, was introduced in order to incorporate more stable tetrazines and improve the pharmokinetic properties in comparison to former modified RGD-conjugates developed. Due to the improved tumor uptake and increased blood circulation of this probe, it was of interest to apply these F-18 labeling substrates to larger proteins and other biomolecules.

Chapter 2 focuses on the development of an assay to quantify antibody degree-of-labeling by in-gel fluorescence. For this project, the aim was to add varying stoichiometric amounts of tetrazine in order to modify antibody with about two tetrazines. Achieving a degree of labeling of about two would allow a suitable amount of tetrazine present for ^{18}F-sTCO conjugation for radiolabeling imaging applications while also avoiding over modification of antibody and causing possible defunctionalization. Lastly, Chapter 3 focuses on the preparation of silver nitrate

complexes of F-18 labeling precursors to enhance long-term storage and stability of these reagents.

Chapter 1

SYNTHESIS OF ^{18}F-PET PROBES VIA TETRAZINE LIGATION

Parts of this chapter are reprinted with permission from: Wang, M.; Svatunek, D.; Rohlfing, K.; Liu, Y.; Wang, H.; Giglio, B.; Yuan, H.; Wu, Z.; Li. Z.; Fox, J. M. *Theranostics* **2016**, *6*, 887-895.

1.1. Introduction

Positron emission tomography (PET) imaging is a non-invasive tool with the capability to track radiolabeled biomolecules *in vivo*.[7] This imaging technique employs radionuclides that emit positrons which collide with electrons and result in detectable γ-rays.[1] The PET scanner is reliant on the production of these photons that leave the site of collision which is then able to convert this information to generate an image. PET imaging has become extensively used in clinical settings to detect and assess a number of diseases and various types of cancers including small-lung, brain, prostate, thyroid, pancreas, breast and many others.[27] Some of the most biologically useful isotopes include C-11, O-15, N-13, Cu-64, Ga-68, I-124 and F-18.[27] Of the isotopes available for these applications, F-18 is the most broadly utilized due to its clinically attractive features including high positron efficiency (nearly 100%), high specific radioactivity and a short half-life (~110 min).[2] These properties are highly favorable in clinical settings due to the lower toxicity and radiation exposure to patients.

One substrate that has had a profound influence on the PET imaging of tumors is ^{18}F-Fluorodeoxyglucose (FDG). In 1980, it was discovered that ^{18}F-FDG accumulates in tumors which led to its evolution as a major clinical tool used in cancer diagnosis.[3] While the use of ^{18}F-FDG has provided a great amount of beneficial information in PET imaging towards the

assessment of cancerous tumors, it is reliant on glycolysis, which causes limitations. Since glucose is metabolized by healthy cells in addition to cancer cells, it is difficult to image small tumors of < 1 cm due to background glycolysis by normal cells.[4] ^{18}F-FDG is also not selective for different types of cancer. In order to generate data with improved resolution and specificity, it is of value to modify proteins and peptides as labeling reagents. While the incorporation of F-18 has many attractive features for this type of application, it also carries limitations due to its short half-life, poor nucleophilicity, and production in low concentrations (~100 nm – 1 μM).[7] These characteristics render challenges for the direct labeling of macromolecules. Due to poor nucleophilicity, the electrophiles that are needed to efficiently combine fluorine to proteins are generally incompatible with biological molecules.[27] Additional attempts have been taken to deliver the radionuclide as a prosthetic group through attachment by an amine, carboxylic acid or thiol binding site on the biomolecule. However, due to the slow rate of conjugation, extended reaction times or excess use of substrate is generally needed in order complete this reaction.[27]

To overcome some of the difficulties associated with F-18 incorporation into proteins, bioorthogonal reactions have been utilized for radiolabeling applications. A widely known method for this purpose has been the Cu-catalyzed cycloaddition of an azide with an alkyne, or more broadly referred to as "click" chemistry.[5] As indicated by the literature, the first employment of "click" chemistry for F-18 PET imaging was demonstrated in 2006 by Marik and Sutcliffe.[6] In their work, the Cu-catalyzed 1,3-dipolar cycloaddition between various fluoroalkynes and azides were utilized to develop ^{18}F-radiolabeled peptides.[6] While this chemistry did provide increased reactivity, specificity and conditions for an indirect way to radiolabel peptides, it also conveys some difficulties. The first is that copper is needed to catalyze this "click" reaction, which is limited for *in vivo* applications due to its cytotoxicity. Secondly, the slow kinetics of this reaction requires high concentrations of the labeling substrate (>1mM), which is not ideal for

macromolecules or radionuclides generally only available in small quantities. The development of a kinetically superior bioorthogonal reaction would allow for a reduction in concentration and remove the need for excess use of substrate.[7] **Table 1.1** shows the importance of fast rates for radiolabeling.[7] As both radionuclides such as F-18 and biological molecules are utilized at low concentrations, fast reaction rates are essential for efficient coupling.[7]

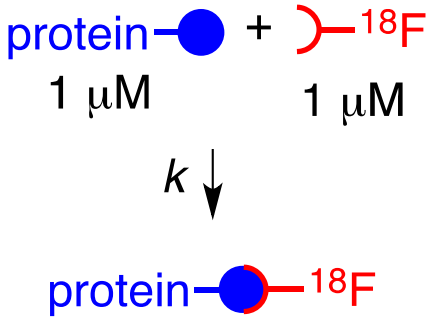

k (L/M•s)	$t_{1/2}$
10^6	1 sec
10^4	1.7 min
10^2	2.8 h
1	12 days
10^{-2}	3 years

Table 1.1: Illustration of the practical importance of fast, bimolecular reactivity for radiolabeling at 1 μM.[7]

One particular very rapid bioorthogonal reaction that has been developed within the Fox lab includes the tetrazine ligation. *Trans*-cyclooctene (TCO) was a substrate of interest while developing this chemistry due to the strain energy associated with this molecule and its ability to drive this reaction as well as the defined chiral structure that makes it attractive for stereocontrolled synthesis.[8] To create a more efficient way to utilize this substrate, the Fox group developed the photoflow apparatus as shown in **Figure 1.1**[8]

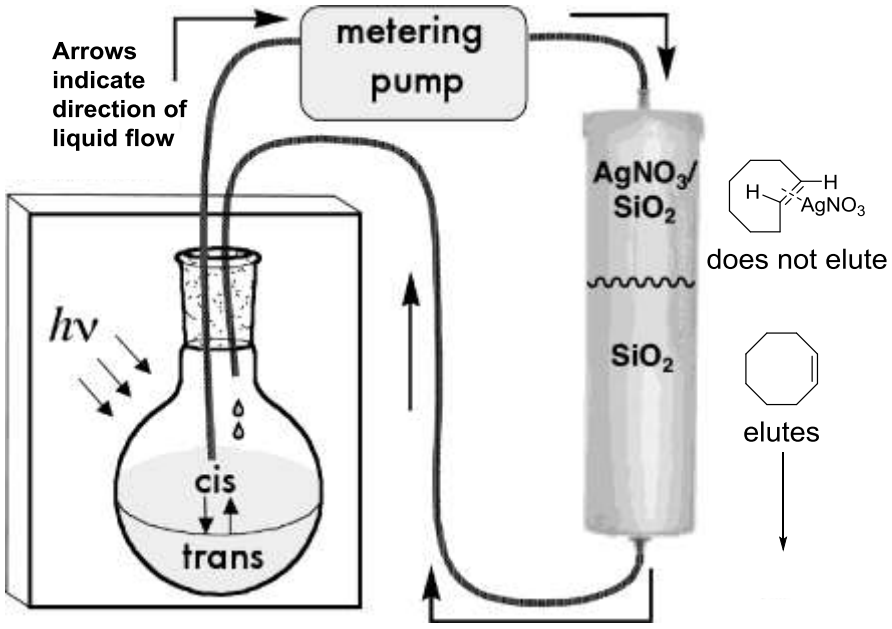

Figure 1.1: Photoflow chemistry apparatus for the synthesis of *trans*-cyclooctene derivatives.[8]

During this reaction, a quartz flask containing a solution of the *cis*-cyclooctene and a singlet sensitizer, methyl benzoate, is subjected to photo irradiation (254 nm) via a Rayonet light source.[8] The solution is then pumped over a bed of silver nitrate embedded silica gel where the *trans*-cyclooctene is selectively retained due to a higher binding affinity and the *cis*-isomer elutes off the column back into the flask.[8] The process is repeated until confirmation by GC determines the reaction is complete. The silica gel containing the TCO is then scraped into a flask and stirred with aqueous NH_4OH to liberate the substrate. Due to the development of this photoflow apparatus, more than fifty TCO derivatives have been prepared on multigram scale.

These TCO substrates then serve as the dienophile to react with tetrazines containing varying electron withdrawing groups (**R**) to create very rapid bioorthogonal chemistry through an inverse electron demand Diels-Alder reaction (**Scheme 1.1**)[9, 10] The tetrazine ligation has been

sufficiently utilized for a number of applications including the creation of biomaterials, the development of interfacial polymers, protein labeling, cell imaging and many others.[11, 12, 20]

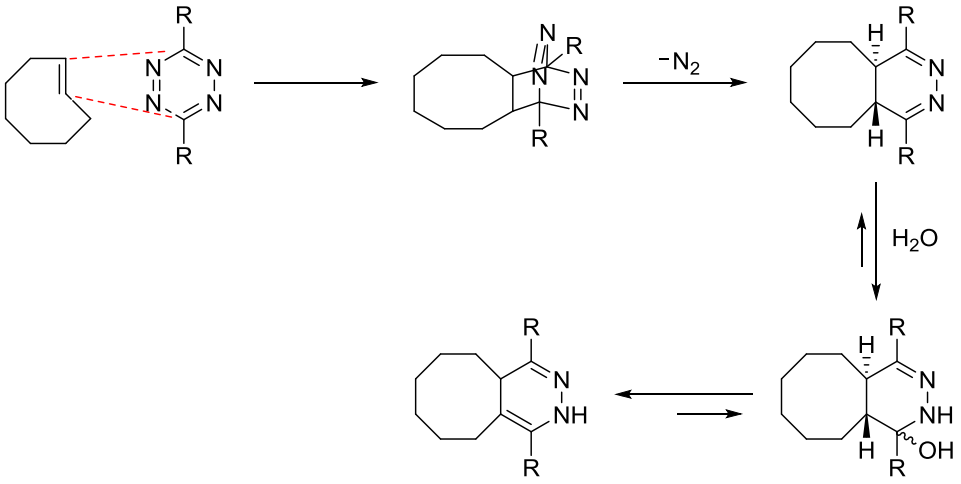

Scheme 1.1: Bioorthogonal reactivity based on the inverse electron demand Diels-Alder reaction (IEDDA).[9]

Due to the bioorthogonality and fast rate of the tetrazine ligation, it makes it an unusually well-suited reaction for radiolabeling applications. In recent work from the Fox lab, the tetrazine ligation was utilized for the development of an F-18 labeled conjugate for *in vivo* PET imaging studies within tumor-bearing mice (**Figure 1.2**).[13-16]

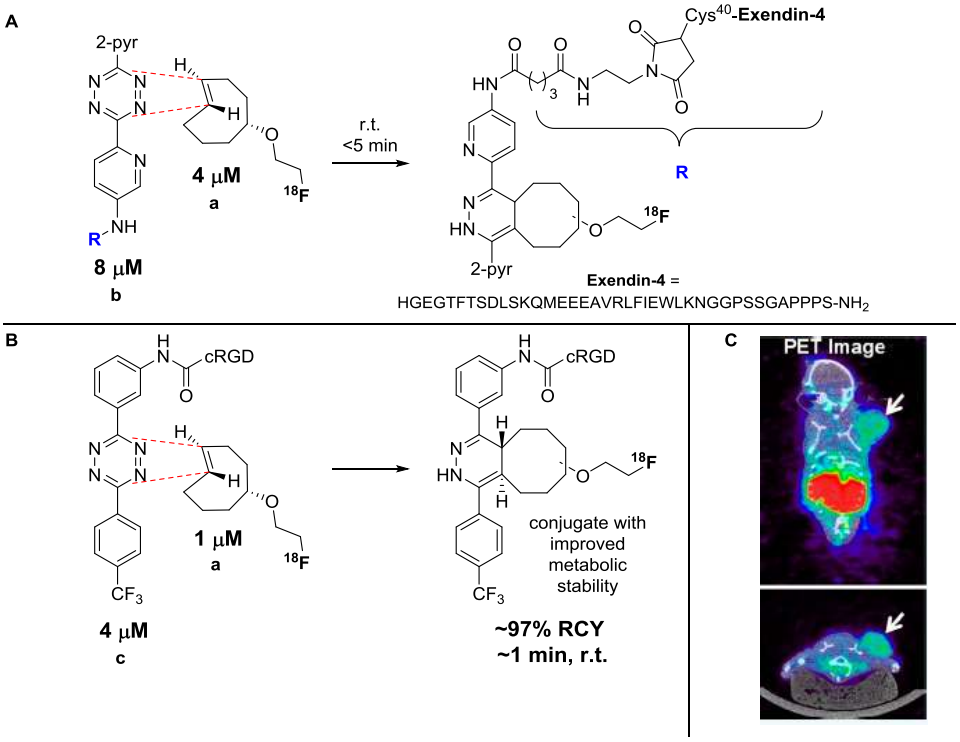

Figure 1.2: The tetrazine ligation with *trans*-cyclooctenes serves as a rapid method for the assembly of biomolecular probe constructs. (**A**) The first generation system for F-18 labeling proceeds with fast kinetics but the Diels-Alder conjugate displays poor metabolic stability.[13, 14] (**B**) Diels-Alder conjugate **a** and diphenyl-*s*-tetrazine derivative **c** displays improved metabolic stability.[15] (**C**) MicroPET scans of human U87MG tumor-bearing mice after 120 min. post injection using ^{18}F-probe between conjugates **a** and **c** .[16]

The first developed system (**Figure 1.2A**), utilized functionalized derivatives of di-2-pyridyl-*s*-tetrazine (**b**) and an ^{18}F-labeled *trans*-cyclooctene (**a**) for the construction of an F-18 labeling probe.[13] The rapid kinetics and low concentrations of these analogs has enabled this system to be suitable for cancer imaging and diabetes monitoring studies.[14, 15] In a recent Bioconjugate Chemistry publication from 2015, substrate **c** was derived from diphenyl-*s*-tetrazine to develop a method that is less rapid in kinetics, but more stable for *in vivo* applications relative to

the first generation system (**Figure 1.2B**).[16] Relative to other RGD peptide conjugates at this time, this tetrazine-TCO ligation is nearly quantitative at concentrations that are more dilute by three orders of magnitude. ^{18}F-labeled TCO **a** has also been explored for pretargeted PET imaging in the brain.[17] The tetrazine ligation has become a significant tool for biomolecular labeling in various areas of research including cell imaging, materials science, *in vivo* reactions, pretargeted imaging, radiolabeling and other applications.[7]

While the tetrazine ligation developed in **Figure 1.2B** displays excellent speed and efficiency for ^{18}F-PET probe construction, there was a desire to improve the pharmokinetics of this system to increase tumor uptake relative to the consumption by surrounding organs observed by PET imaging (**Figure 1.2C**). In order to employ a broader range of tetrazines, a kinetically faster ligation was needed. Of the TCO's explored within the Fox group, the conformationally strained dienophile, 'sTCO', is the most reactive dienophile described to date. For this substrate, rate constants as fast as 3.3 x 10^6 $M^{-1}s^{-1}$ have been measured (**Table 1.2**).[18]

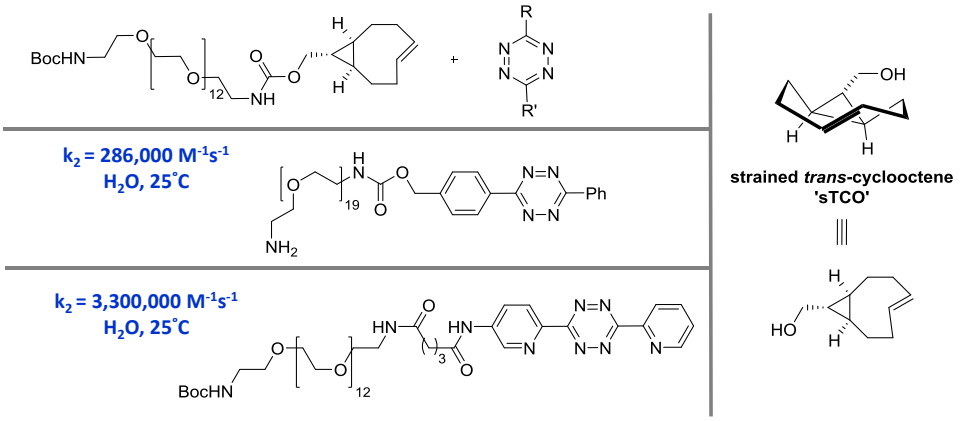

Table 1.2: The conformationally strained sTCO is the most reactive dienophile described to date, with rate constants of up to 3.3 x 10^6 $M^{-1}s^{-1}$ for room temperature conjugations in water.[18]

Based on these results, it was hypothesized that this dienophile could display superior kinetics in tetrazine ligation and serve as a unique reactive tool for the instantaneous construction of protein-radiolabeled conjugates. Described in this work is the development of a new radiotracer, ^{18}F-sTCO, for the assembly of PET imaging probes via tetrazine ligation. This project was a collaborative effort between a Ph. D student from Tu Wien, Dennis Svatunek, Dr. Zibo Li's group at UNC and the Fox group. Dennis and I conducted the synthesis for this collaboration while Dr. Li's group completed the radiochemistry and performed PET imaging studies within a mouse system.

1.2 Results and Discussion

The desired ^{18}F-sTCO substrate was initially developed using synthetic methodology previously established within the Fox lab starting from commercially available reagent, 1,5-cyclooctadiene (**Scheme 1.2**).[19] From this reagent, the *cis*-alcohol **1** can be produced in two steps and then photoisomerized to the *trans*-isomer **2** in 81% yield using the flow reactor previously described (**Figure 1.1**).[8] Alkylation of **2** using a bis-tosylate mini-PEG linker provided sTCO-tosylate **3** in 28% yield (**Scheme 1.2**). Treatment of **3** with TBAF in anhydrous THF gave the ^{19}F-labeled substrate **4** to be used as the HPLC standard in 76% yield. To develop the radiolabeled substrate, sTCO-precursor **3** (182 mM) was also treated with ^{18}F-TBAF in acetonitrile at 85 °C for 10 min by Dr. Li's group.

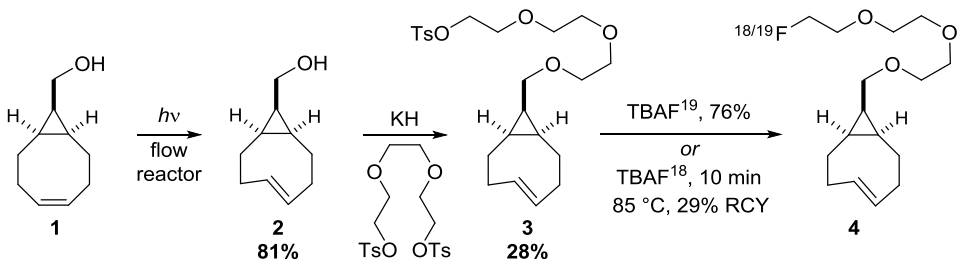

Scheme 1.2: Synthesis of *syn*-sTCO labeling precursor **3**, cold standard **^{19}F-4** and radiotracer **^{18}F-4**.[19]

They were able to obtain radiolabeled **^{18}F-4** in 29.3 + / - 5.1% isolated yield with 99% radiochemical purity after HPLC purification (**Figure 1.3**). The specific activity was determined to be 2.1 + / - 0.8 Ci/μmol. For these reactions, it was determined that the concentration was important, as running the reaction at 91 mM gave **^{18}F-4** in only 9.3 + / - 2.4% isolated yield. Prior to reacting **^{18}F-4** with additional substrates to form the PET imaging conjugate, the *in vitro* stability was tested by the Li group. The first study showed that after incubation in 1x PBS, the radiochemical purity remained at 97.5% and 97.3% after 1 and 2 hour time points. An additional stability study using fetal bovine serum demonstrated that 74% radiochemical purity of **^{18}F-4** remained after 1 hour. The results from this data verified that **^{18}F-4** would be sufficiently stable for constructing ^{18}F-PET probes in aqueous media.

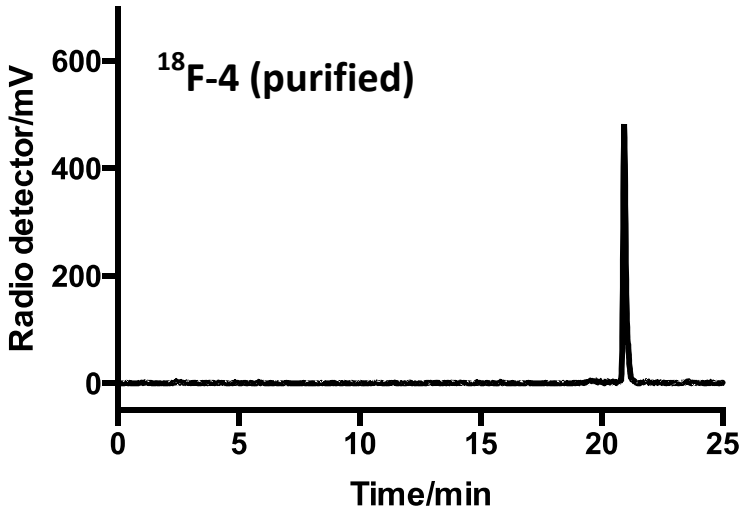

Figure 1.3: Radio-analysis of **^{18}F-4** after purification by HPLC.

Solely for kinetic reasons, the *syn*-alcohol was moved forward relative to the *anti*-isomer due to slightly faster reactivity with the diphenyl-*s*-tetrazine (**Figure 1.4**). For these data points, the stopped-flow experiments were conducted by Dennis while I worked up the data in Prism Software and generated the kinetic figures displayed (**Figure 1.4** & **Figure A1**). The second order rate constant was measured under pseudo-first order conditions using an excess of the sTCO diastereomer (***syn*** or ***anti***) and by following the exponential decay of absorbance due to the tetrazine chromophore at 298 nm using an SX 18MV-R stopped-flow spectrophotometer (Applied Photophysics Ltd.). For each run, equal volumes of 45:55 water : methanol solutions of sTCO and PEGylated tetrazine **6** were mixed in the stopped flow device. Reactions were carried out with tetrazine **6** at 0.05 mM and final concentrations of 0.245, 0.49, 0.98 and 1.47 mM for the *syn*-diastereomer (**Figure A1**). Similarly, reactions were carried out with tetrazine **6** at 0.05 mM and final concentrations of 0.25, 0.50, 1.00 and 1.50 mM for the *anti*-diastereomer (**Figure A1**). A total of 400 data points were recorded over a period of 1 second and each sample was performed in sextuplicate at 298 K. The k_{obs} was determined by nonlinear regression analysis of the data points using Prism software (v. 6.00, GraphPad Software Inc.). The rate constant for the *syn*-diastereomer with tetrazine **6** was k_2 3.7 x 10^4 (+/- 0.1 x 10^3) $M^{-1}s^{-1}$ and the *anti*-diastereomer was k_2 3.3 x 10^4 (+/- 0.1 x 10^3) $M^{-1}s^{-1}$. Due to the observed higher reactivity of the *syn*-sTCO, it was chosen for further development in ^{18}F-PET probe assembly.

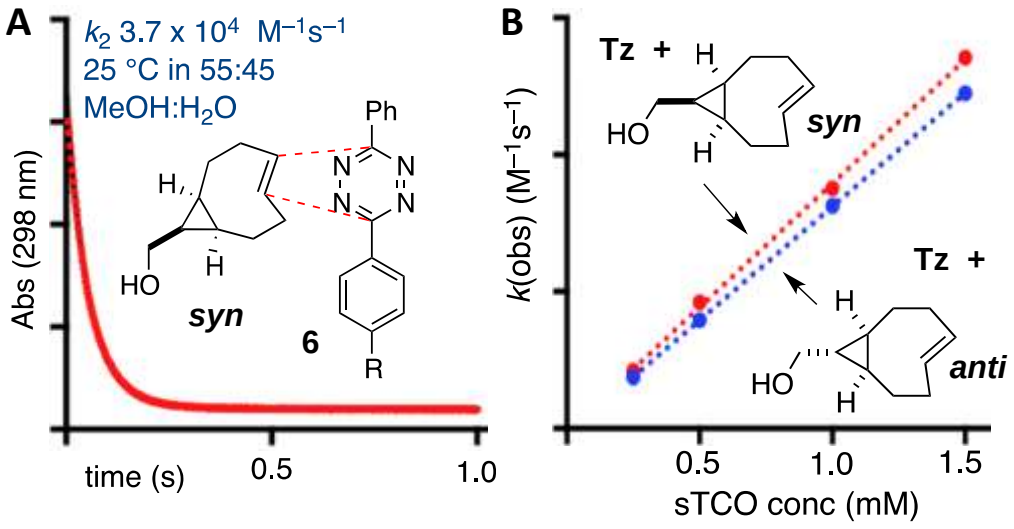

Figure 1.4: Rapid bioconjugation. (**A, B**) Rate constants for the *syn*- and *anti*- diastereomers of sTCO were measured in mixed aqueous/organic media. (**A**) Kinetic data for the reaction of a syn-sTCO (0.49 mM) and a water soluble diphenyltetrazine (0.05 mM). (**B**) The sTCO *syn*-diastereomer is slightly more reactive than the *anti*-diastereomer.

As shown in **Scheme 1.3**, the diphenyl-*s*-tetrazine-RGD conjugate was prepared from carbonate **5**[20] coupled with a mini-PEG amino acid to improve water stability as intermediate **6**. The tetrazine-PEG-amino acid **6** was then transformed to the NHS ester and conjugated with cyclic peptide RGDyK to give **7** in high yield (99%) after purification by HPLC (**Figure A2**). Prior to this work, RGDyK cyclic peptide sequence had been used with modification to image integrin $\alpha_v\beta_3$.[21-24] This integrin which is upregulated on the endothelial surface of tumor blood vessels has been linked to tumor progression and metathesis.[25] For these experiments, tumors were generated from U87MG glioblastoma cells and imaged via PET scans within a mouse system using the F-18 construct developed during this project.

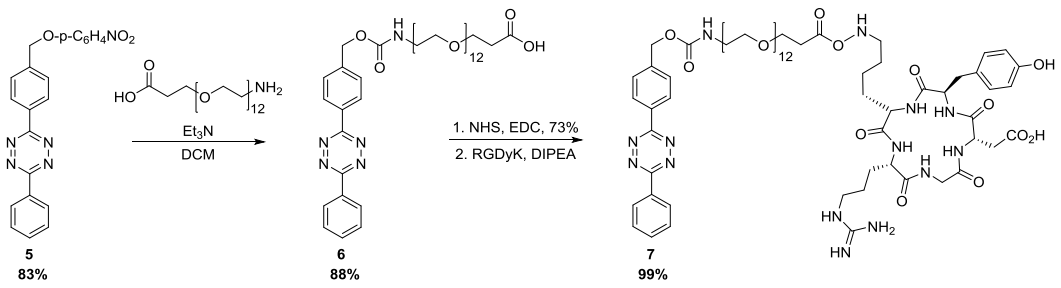

Scheme 1.3: Synthesis of cyclic RGD-diphenyl-*s*-tetrazine conjugate **7**.

In order to construct the F-18 probe, the Li group combined ^{18}**F-4** with **7** (700 μM) to produce ^{18}**F-8** as a mixture of isomers (**Scheme 1.4, Figure 1.5A)**. Upon initial assay, the ^{18}**F-4** starting material was completely consumed (<5 min.). An additional experiment where reducing the concentration of **7** (33 μM) led to an inversion in stoichiometry and resulted in the complete consumption of the modified RGD conjugate and unreacted ^{18}**F-4**. The observation from this experiment demonstrates the high efficiency and rate of this reaction even when the radiolabeled substrate is used in excess. Conjugate **8** could be obtained in a 91% radiochemical yield with 99% purity after purification by HPLC (**Figure 1.5B**). The specific activity was determined to be 0.91 + / - 0.20 Ci/μmol. The *in vitro* stability of **8** was studied where the adduct was incubated in PBS buffer at 37 °C for 2 hours and retained 98.5% of its chemical purity (**Figure 1.5B**). It was also found that **8** was stable in fetal bovine serum with retention of 96.7% and 94.5% purity at 2 and 4 hours post incubation.

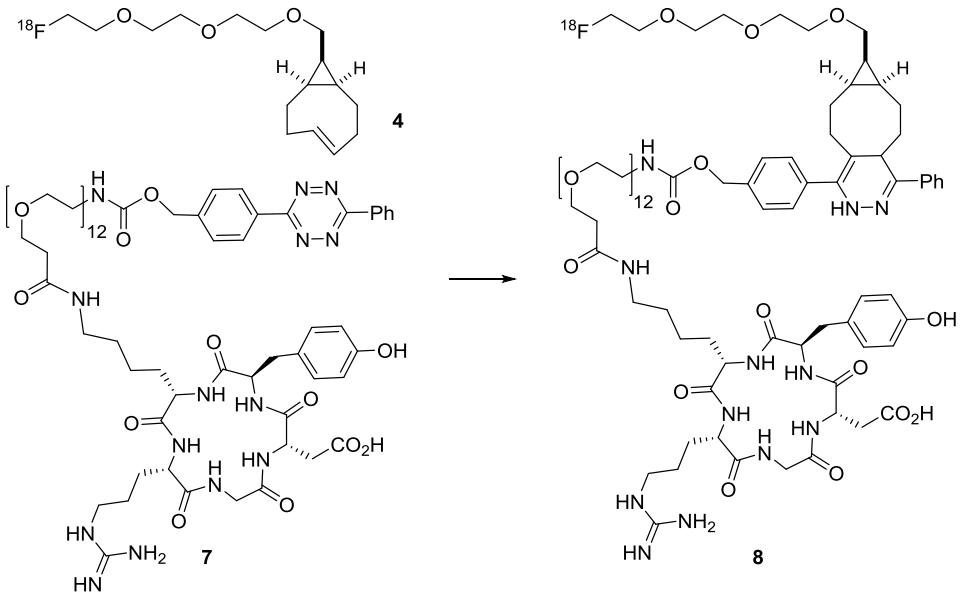

Scheme 1.4: Conjugation of **^{18}F-4** with RDG-tetrazine **7** to produce conjugate **^{18}F-8** as a mixture of isomers.

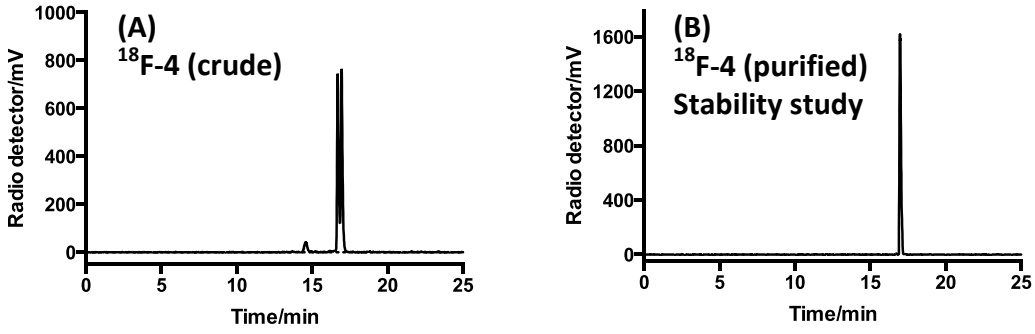

Figure 1.5: Radio-HPLC analyses. (**A**) Combination of **^{18}F-4** with **7** gives two major isomer adducts. (**B**) The slow eluting isomer of **^{18}F-8** after purified by HPLC, incubation in PBS for 2 h at 37 °C and reanalysis.

1.2.1 *In Vivo* Imaging Studies

Animal procedures were performed by the Li group according to a protocol approved by the UNC Instutional Animal Care and Use Committee. Human U87MG tumor-bearing mice were anesthetized using 2% isoflurane and injected with 3.7 MBq (100 μCi) of **^{18}F-8** via the tail vein. Static microPET scans were then performed for 10 min. at time-points 0.5, 1.0, 2.0 and 4.0 h post injection. The tumor uptake was 5.3 +/- 0.2, 6.9 +/- 0.5, 7.5 +/- 0.8 and 8.9 +/- 0.5% ID/g at the 0.5, 1.0, 2.0 and 4.0 h respective time points (**Figure 1.6A**). As early as 30 min. p.i., high tumor accumulation was observed with good tumor to background contrast. The PET scan at 4.0 h p.i. showed the tumor became the brightest spot with a tumor-to-liver and tumor-to-kidney ratio of 1.6 and 2.4, respectively. A blocking experiment was also conducted to confirm the specificity of **^{18}F-8** by co-injecting the radiotracer with an excess amount of cRGDyK (200 μg). As observed in **Figure 1.6B**, the tumor uptake dropped to 4.8 +/- 0.3% ID/g at 1 h post injection in the presence of non-radiolabled cRGDyK peptide. Due to the presence of PEGylated chains on the **^{18}F-8** conjugate, the non-radiolabeled and non-PEGylated peptide did not completely block the signal due to being more rapidly cleared in the mouse system. However, the signal in the presence of blocking cRGDyK was still significantly lower ($P < 0.05$) than that observed without a blocking agent.

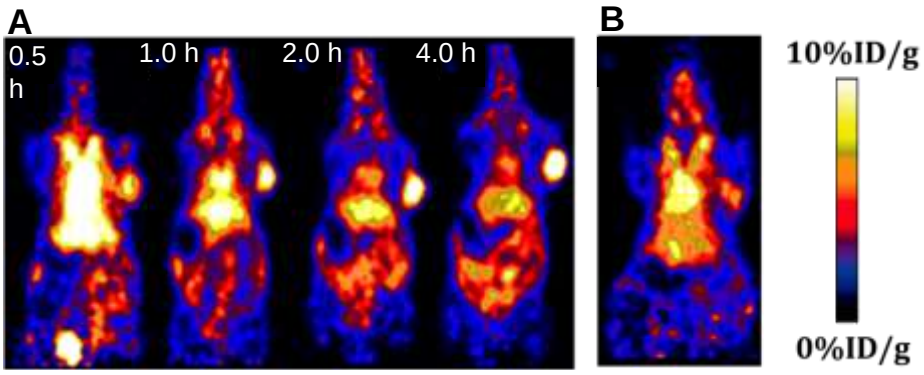

Figure 1.6: (**A**) Small animal PET images of mice bearing U87 xenograft, injected with ^{18}**F-8** and imaged 0.5 h, 1.0 h, 2.0 h and 4.0 h post injection, respectively. (**B**) A 'blocking' experiment in which cyclic RGDyK peptide (200 μg) was injected prior to the injection of ^{18}**F-8**, with imaging at 1.0 h post injection.

The quantitative biodistribution derived from small-animal PET images were evaluated by the Li group as demonstrated in **Figure 1.7**. The inclusion of mini-PEG spacers on both the sTCO and tetrazine during the construction of **8** resulted in a biodistribution profile that was significantly improved relative to previous TCO-tetrazine based probes which lacked a PEG spacer (**Figure 1.2**). Tumor uptake in addition to blood circulation increased for this new sTCO-tetrazine conjugate.

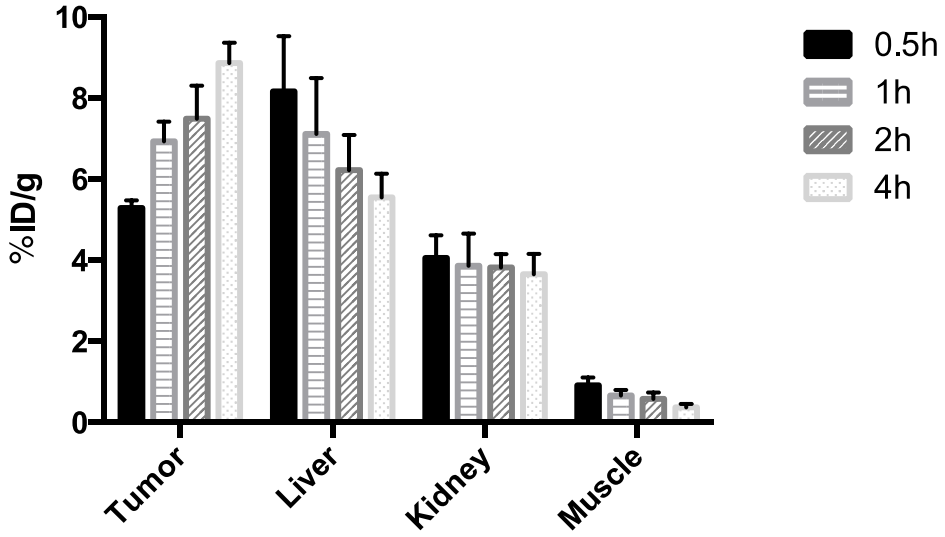

Figure 1.7: Tumor and major organ radioactivity accumulation quantification from a static scan at 0.5, 1.0, 2.0, and 4.0 h post injection of ^{18}**F-8** into U87MG tumor model. Data are expressed as average +/- SD.

1.3 Conclusions

Due to the low concentration and short time scale that is intrinsic to F-18 labeling of proteins, the fast kinetics and bioorthogonality of the tetrazine-TCO ligation provides a clear benefit over conventional radiolabeling methods. As observed in the prior system (**Figure 1.2**), highly reactive tetrazines were required in order to obtain rapid reactivity at micromolar concentrations. However, the conjugates only had moderate stability *in vivo*. In this work, the development of a new system focuses on the incorportation of a conformationally strained *trans*-cyclooocten (sTCO), a dienophile that is approximately 2 orders of magnitude more reactive than conventional TCO substrates. The second order rate constant was measured for two sTCO-diastereomers, with the *syn*-isomer being slightly more reactive and therefore chosen for further development. The superior reactivity of ^{18}F-sTCO ($> 10^4$ $M^{-1}s^{-1}$) allowed for the use of more stable diphenyl-*s*-tetrazines, giving rise to Diels-Alder conjugates which are known to to possess improved *in vivo* stablity.[16] The substrates used for the assembly in this F-18 PET imaging probe were also equipped with mini-PEG groups to improve both the water stability and pharmokinetic properties. As opposed to previous systems, this radiolabeled cyclic RGD based probe experienced higher levels of tumor uptake and increased blood circulation in tumor-bearing mice. Due to the exceptional kinetics, improved tumor accumulation and prolonged blood circulation of **^{18}F-8**, it is expected that this F-18 system will be suitable for broad use in probe construction of proteins, pretargeted imaging and treatment applications.

1.4 Experimental Section

1.4.1 General Considerations

All reactions were carried out in glassware that was flame-dried under vacuum and cooled under nitrogen. All commercially available reagents and solvents were used as received. (rel-1R,8S,9S,4Z)-Bicyclo[6.1.0]non-4-ene-9-ylmethanol and 4-nitrophenyl 4-(6-phenyl-1,2,4,5-tetrazin-3-yl)benzyl carbonate were prepared following known procedures.[19,20] Reactions were monitored by thin layer chromatography (TLC) performed on SiliCycle silica gel GF 250 μm plates and were visualized with ultraviolet (UV) light (254 nm) and/or $KMnO_4$ staining. Flash chromatography was performed using normal phase SiliCycle silica gel (40-63D, 60Å). Deactivated silica gel was prepared by treating silica gel with $EtSiCl_3$.[26] ^1H, ^{13}C and ^{19}F nuclear magnetic resonance (NMR) chemical shifts are reported in ppm relative to $CHCl_3$, CH_2Cl_2 and MeOH (i.e. ^1H NMR δ = 7.26 and ^{13}C NMR = 77.0, ^1H NMR = 5.32 and ^{13}C NMR = 54.0, ^1H NMR = 3.31 and ^{13}C NMR = 49.1). These synthetic procedures and corresponding spectral data could also be viewed in a recent Theranostics publication.[7]

1.4.2 Synthetic Procedures

(rel-1R,8S,9S,4E)-Bicyclo[6.1.0]non-4-ene-9-ylmethanol (2)

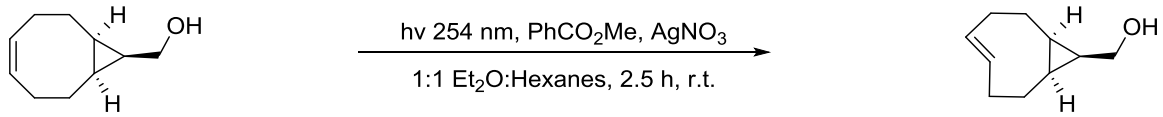

1 **2**

The general photoisomerization procedure was followed using **1** (395 mg, 2.59 mmol) in 1:1 ether/hexanes (250 mL), methyl benzoate (705 mg, 5.18 mmol) and dodecane (491 mg, 2.88 mmol, standard for GC monitoring) in a 250 mL quartz tube. A 50 g Biotage® SNAP column was filled with normal silica gel (2.5 inches) and the remaining space was packed with 10% silver impregnated silica (5.70 g). The column was connected to a pump and flushed with 1:1 ether/hexanes (250 mL). Irradiation was carried out at 254 nm for 2.5 h at which GC monitoring showed no more starting material. The column was flushed with 1:1 ether/hexanes (250 mL) and dried under air flow. The silica was placed into a flask and stirred in ammonium hydroxide (200 mL) and dichloromethane (200 mL) for 10 min. The silica was filtered and washed with additional ammonium hydroxide (100 mL) and dichloromethane (100 mL). The phases were separated and the aqueous layer was extracted an additional three times. The combined organic layers were washed twice with water, dried over Na_2SO_4, filtered and concentrated by rotary evaporation. Purification by column chromatography (25%, EtOAc : Hexanes) to yield 318 mg (2.09 mmol, 81%) of compound **2** as a colorless oil which was stored as a solution in MeOH at -15 °C. ^{1}H NMR (600 MHz, CD_3OD) δ: 5.88 (ddd, *J* = 16.2, 9.3, 6.2 Hz, 1H), 5.16 (dddd, *J* = 16.7, 10.6, 3.9, 1.1 Hz, 1H), 3.50 (d, *J* = 7.7 Hz, 2H), 2.31 (dtd, *J* = 11.4, 3.7, 2.4 Hz, 1H), 2.28 (ddd, *J* = 12.5, 8.4, 6.9 Hz, 1H), 2.21 – 2.15 (m, 1H), 2.13 – 2.09 (m, 1H), 1.96 – 1.86 (m, 2H), 1.20 (dt, *J* = 9.1, 7.7 Hz, 1H), 1.09 (tdd, *J* = 12.9, 11.2, 7.1 Hz, 1H), 0.85 – 0.71 (m, 2H), 0.60 (dtd, *J* = 13.0, 8.8, 4.6 Hz, 1H), (small peaks attributable to impurities were detected by ^{1}H NMR at 5.49, 4.09, 2.01, 1.29,1.24 and 0.90 ppm). ^{13}C NMR (151 MHz, CD_3OD) δ 139.4, 132.3, 59.5, 35.3, 34.8, 28.6, 28.3, 21.7, 20.2, 19.2; HRMS (EI) [M+H] *m/z*: calcd for $C_{10}H_{16}O$: 152.1201; found: 152.1181.

2-(2-(2-((*syn*-(*E*)-bicyclo[6.1.0]non-4-en-9-yl)methoxy)ethoxy)ethoxy)ethyl 4-methylbenzenesulfonate (3)

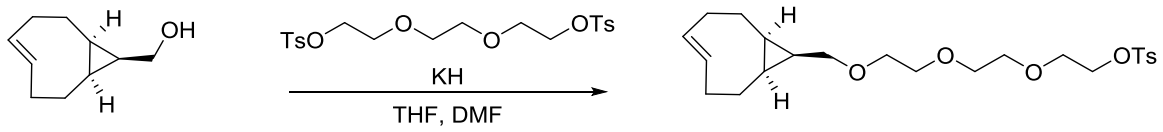

2 **3**

Triethylene glycol bis(*p*-toluenesulfonate) (972 mg, 2.12 mmol) was added into a flame-dried round bottom flask and dissolved in anhydrous THF (6.0 mL, 0.35M) and DMF (0.6 mL, 3.53M). **2** (100mg, 0.66 mmol) was added followed by potassium hydride (210 mg, 50% in paraffin, 2.63 mmol). The mixture was stirred at room temperature for 16 h after which saturated aqueous NH_4Cl solution was added followed by ether. The phases were separated and the aqueous layer was extracted an additional three times. The combined organic layers were dried over Na_2SO_4, filtered and concentrated by rotary evaporation. Purification by column chromatography (25 - 50%, EtOAc : Hexanes) yielded 85 mg (0.19 mmol, 30%) of desired compound **3** as a colorless oil which was stored as a solution in MeOH at -15 °C. ^{1}H NMR (600 MHz, CD_3OD) δ: 7.80 (d, *J* = 8.3 Hz, 2H) 7.45 (d, *J* = 8.4 Hz, 2H), 5.86 (ddd, *J* = 16.2, 9.3, 6.3 Hz, 1H), 5.16 (dddd, *J* = 16.8, 10.6, 3.9, 1.1 Hz, 1H), 4.18-4.12 (m, 2H), 3.68-3.34 (m, 2H), 3.60-3.52 (m, 8H), 3.46 – 3.41 (m, 2H), 2.46 (s, 3H), 2.34-2.27 (m, 1H), 2.26-2.19 (m, 1H), 2.19-2.11 (m, 1H), 2.11-2.04 (m, 1H), 1.98-1.84 (m, 2H), 1.30-1.19 (m, 1H), 1.14-1.01 (m, 1H), 0.87-0.69 (m, 2H) 0.65-0.55 (m, 1H), (small peaks attributable to impurities were detected by ^{1}H NMR at 4.63, 4.09, 2.01 and 1.24 ppm) ; ^{13}C APT NMR (100.6 MHz, CD_3OD) δ: 146.5, 139.4, 134.6, 132.4, 131.2, 129.2, 73.1, 71.7,

71.7, 71.6, 71.0, 69.9, 69.1, 35.5, 34.8, 28.8, 28.4, 21.7, 20.3, 19.3, 19.2, (a small peak attributable to dichloromethane was detected by ^{13}C at 54.9 ppm); HRMS (LIFDI-TOF) *m/z*: $[M]^+$ Calcd for $C_{23}H_{34}O_6S^+$ 438.2076; Found 438.2066.

syn-(_E_)-9-((2-(2-(2-fluoroethoxy)ethoxy)ethoxy)methyl)bicycle[6.1.0]non-4-ene (^{19}F-4)

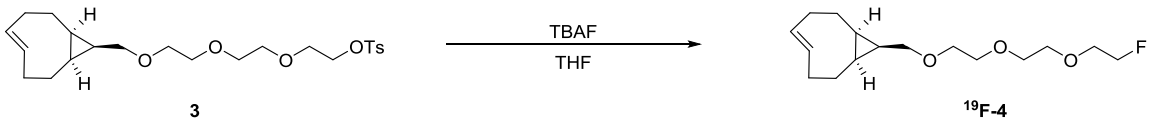

Tosylate **3** (10 mg, 0.02 mmol) was charged into a 4 dram vial and TBAF (0.5 mL, 1.0 M in THF) was added via syringe. The mixture was heated to 60 °C for 3.5 h and subsequently cooled to room temperature. The mixture was diluted with ethyl acetate, washed with saturated aqueous $NaHCO_3$ and dried over Na_2SO_4. The solution was filtered and concentrated by rotary evaporation. Purification by column chromatography (25%, EtOAc : Hexanes) yielded 5 mg (0.02 mmol, 76%) of **^{19}F-4** as a colorless oil that was stored as a solution in MeOH at -15 °C. ^{1}H NMR (600 MHz, CD_3OD) δ: 5.87 (ddd, *J* = 16.2, 9.3, 6.2 Hz, 1H), 5.17 (ddd, *J* = 14.0, 10.6, 3.8 Hz, 1H), 4.52 (dt, J_{CF} = 48 Hz, J_{HH} = 4.1 Hz, 2H), 3.72 (dt, J_{CF} = 30.1 Hz, J_{HH} = 4.0 Hz, 2H), 3.68-3.59 (m, 6H), 3.59-3.54 (m, 2H), 3.44 (d, *J* = 7.5 Hz, 2H), 2.34-2.28 (m, 1H), 2.28-2.21 (m, 1H), 2.19-2.13 (m, 1H), 2.11-2.06 (m, 1H), 1.99-1/84 (m, 2H), 1.27-1.21 (m, 1H), 1.14-1.04 (m, 1H), 0.86-0.80 (m, 1H), 0.79-0.71 (m, 1H), 0.65-0.57 (m, 1H), (small peaks attributable to the cis isomer (5.61 ppm) and an impurity (1.29, 0.90 ppm) were also detected by ^{1}H NMR); ^{13}C APT NMR (100.6 MHz, MeOD) δ: 139.4, 132.4,

84.2 (d, JCF = 168 Hz), 71.82, 71.76, 71.74 (d, JCF = 20 Hz), 71.65, 71.0, 69.1, 35.5, 34.8, 28.8, 28.4, 20.3, 19.4, 19.3; ^{19}F NMR (376 MHz, CD_3OD) δ: -224.7 (tt, *J* = 48.1, 30.0 Hz); HRMS (Orbitrap) *m/z*: $[M + Na]^+$ Calcd for $C_{16}H_{27}FO_3Na$ 309.18364; Found 309.18453.

3-oxo-1-(4-(6-phenyl-1,2,4,5-tetrazin-3-yl)phenyl)-2,7,10,13,16,19,22,25,28,31,34,37,40-tridecaoxa-4-azatritetracontan-43-oic acid (6)

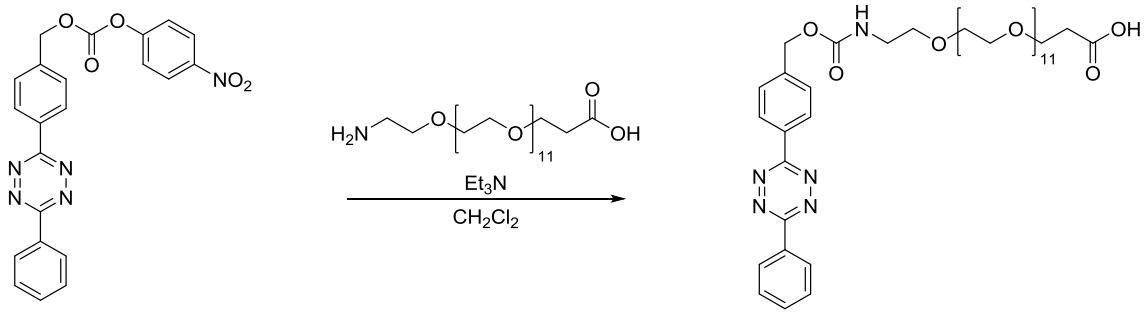

5 **6**

4-nitrophenyl 4-(6-phenyl-1,2,4,5-tetrazin-3-yl)benzyl carbonate (**5**) (43 mg, 0.10 mmol) and PEG12-Amino acid (31 mg, 0.05 mmol) were dissolved in anhydrous dichloromethane (4.0 mL, 0.01 M). Triethylamine (13.8 µL) was added and the reaction was stirred at room temperature for 30 h. 1N HCl (5 mL) was added and the aqueous phase was extracted with dichloromethane (3x). The combined organics were dried over Na_2SO_4, filtered and concentrated by rotary evaporation. The crude was purified by column chromatography using deactivated silica gel (2.50 g, 0 - 5% MeOH : DCM) to yield 40 mg (0.04 mmol, 88%) of **6** as a purple solid. mp: 39 - 40 °C; ^{1}H NMR (400 MHz, $CDCl_3$) δ: 8.67-8.61 (m, 4H), 7.70-7.59 (m, 5H), 5.58 (t, J = 5.8 Hz, 1H), 5.22(m,

2H), 3.73 (t, J = 5.8 Hz, 2H), 3.66-3.54 (m, 48H), 3.39 (q, 5.4 Hz, 2H), 2.60 (bs, 2H); ^{13}C NMR (100 MHz, $CDCl_3$) δ: 173.3, 164.1, 163.8, 156.5, 141.8, 132.9, 131.8, 131.4, 129.5, 128.6, 128.2, 128.1, 70.8, 70.7 – 70.5 (19 C's), 70.4, 70.3, 70.1, 66.7, 66.0, 41.1, 35.1 (a peak attributed to CH_2Cl_2 was observed at 54 ppm); HRMS (LIFDI-TOF) *m/z*: $[M + Na]^+$ Calcd for $C_{43}H_{65}N_5O_{16}Na$ 930.4324; Found 930.4336.

2,5-dioxopyrrolidin-1-yl 3-oxo-1-(4-(6-phenyl-1,2,4,5-tetrazin-3-yl)phenyl) 2,7,10,13,16,19,22,25,28,31,34,37,40-tridecaoxa-4-azatritetracontan-43-oate (6a)

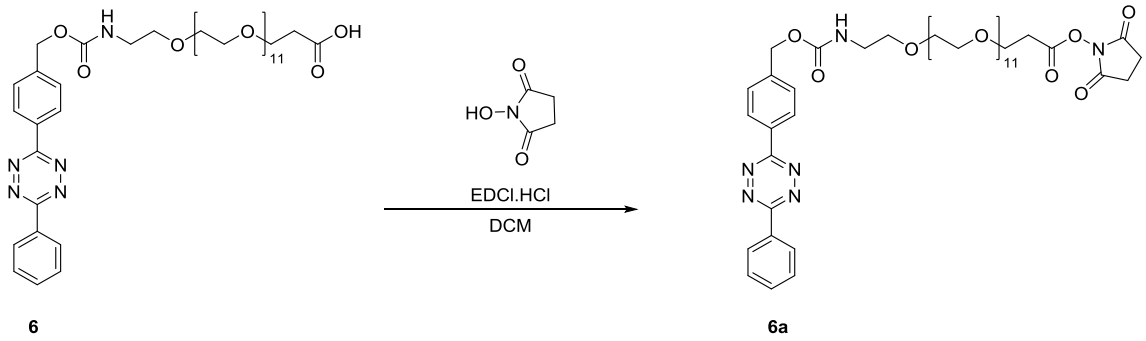

6 6a

Acid **6** (24 mg, 0.0264 mmol), N-hydroxysuccinimide (NHS) (5.0 mg, 0.0434 mmol) and 1-ethyl-3-(3-dimethylaminopropyl)carbodiimide hydrochloride (EDCl) (8.0 mg, 0.0417 mmol) were added to a flame-dried round bottom flask. The mixture was dissolved in anhydrous dichloromethane (2.0 mL, 0.02 M) and stirred at room temperature for 16 h. The solution was directly applied to a column of deactivated silica gel (2.50 g) and washed with large amounts of dichloromethane after which product was eluted with 5% MeOH : DCM. Further purification using HILIC (2.50 g silica gel, 5% H_2O : MeOH) yielded 19 mg (0.02 mmol, 72%) of **6a** as a purple solid. mp: 37 - 39

°C; ^{1}H NMR (400 MHz, CD_2Cl_2) δ: 8.67-8.60 (m, 4H), 7.70-7.59 (m, 5H), 5.54 (bs, 1H, NH), 5.22 (s, 2H), 3.83 (t, J = 6.3 Hz, 2H), 3.67-3.52 (m, 48H), 3.39 (m, 2H), 2.88 (t, J = 6.3 Hz, 2H), 2.84-2.76 (bs, 4H); ^{13}C NMR (100 MHz, CD_2Cl_2) δ: 169.5, 167.3, 164.4, 164.2, 156.5, 142.5, 133.0, 132.3, 131.8, 129.7, 128.7, 128.3, 128.2, 71.0, 70.9 – 70.7 (20 C's), 70.3, 66.0, 41.4, 32.5, 26.0; HRMS (LIFDI-TOF) *m/z*: $[M + Na]^+$ Calcd for $C_{47}H_{68}N_6O_{18}Na$ 1027.4488; Found 1027.4487, : $[M + K]^+$ Calcd for $C_{47}H_{68}N_6O_{18}K$ 1043.4227, Found 1043.4200.

RGDyK-Tz (7)

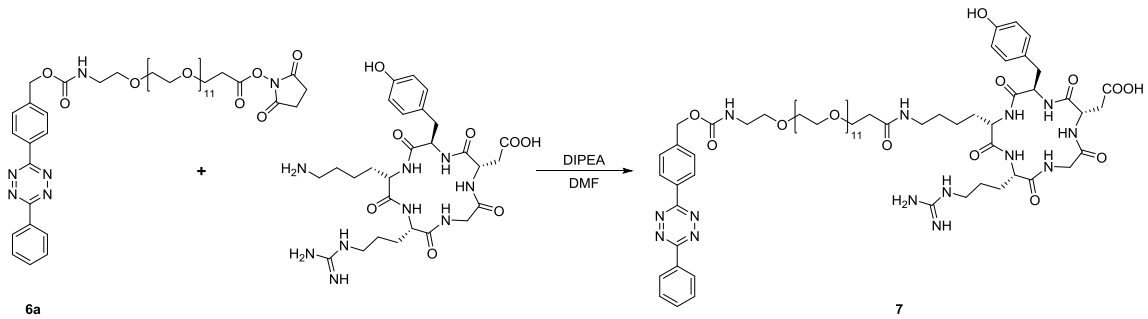

RGDyK (3.0 mg, 0.0048 mmol) was added to a 4 dram vial followed by TzPEG12NHS (**6a**) (10 mg, 0.0099 mmol) as a solution in anhydrous dimethylformamide (400 μL, 0.01 M). *N*,*N*-diisopropylethylamine (3.0 mg, 0.02 mmol) was added as a solution in anhydrous dimethylformamide (100 μL, 0.20 M) and the reaction was allowed to stir at room temperature for 18 h. H_2O was added and the solvents were removed via freeze drying. The residue was purified by RP HPLC to yield 7.2 mg (**7**) (0.005 mmol, 99 %) as a pink solid. HRMS (LIFDI-TOF) *m/z* $[M + Na]^+$ Calcd for $C_{70}H_{104}N_{14}O_{23}Na$ 1531.7296; Found 1531.7279.

RGDyK-Tz-sTCOPEGF (8)

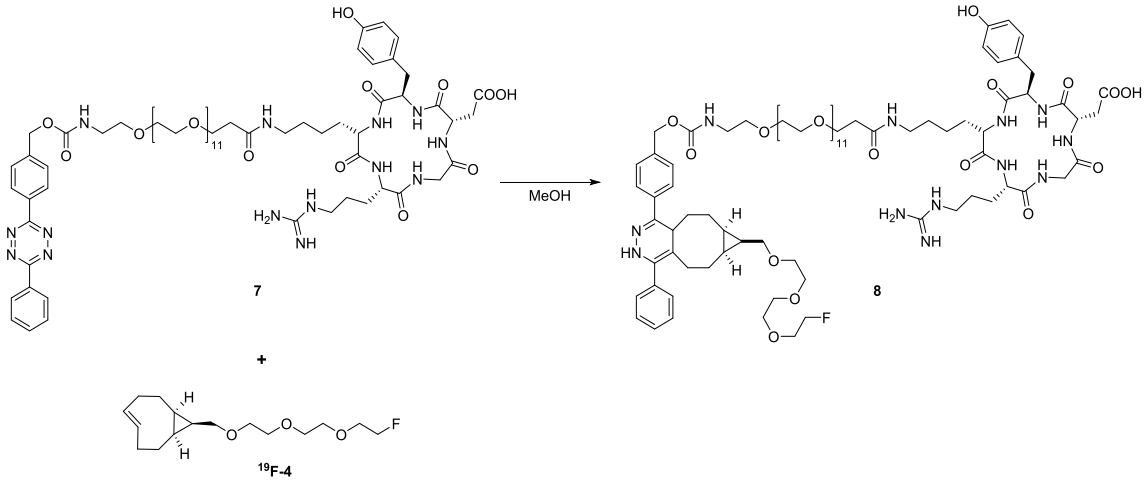

Tetrazine-RGD conjugate (**7**) (0.3 mg, 0.0002 mmol) was dissolved in methanol (0.5 mL) and sTCOPEGF (**^{19}F-4**) (23 μL of a 2.5 mg/mL solution in MeOH, 0.06 mg, 0.0002 mmol) was added dropwise. The reaction was monitored by UV/Vis and was complete within 1 min. The product (**8**) was purified by reverse phase HPLC (C-18 column, 10% ACN + 0.1% formic acid to 100% ACN + 0.1% formic acid).

1.4.3 General procedure for stop-flow kinetic analysis of sTCO's and diphenyl-*s*-tetrazine at variable concentrations

For these experiments, Dennis completed the stopped-flow reactions while I worked up the data in Prism Software and generated the kinetic figures as shown. The reaction between sTCOs (***syn*** & ***anti***) and the PEGylated tetrazine **6** was measured under pseudo-first order conditions in water : methanol 45:55 by following the exponential decay of the tetrazine at 298 nm over time using an SX 18MV-R stoppedflow spectrophotometer (Applied Photophysics Ltd.). Solutions were prepared

for the sTCO concentrations (see table below, water : methanol 45:55) and the tetrazine (0.1 mM in water : methanol 45:55) and thermostatted in the syringes of the spectrophotometer before measuring. An equal volume of each was mixed by the stopped flow device (resulting concentrations shown in the table below). 400 data points were recorded over a period of 1 second, and performed in sextuplicate at 298 K. The k_{obs} was determined by nonlinear regression analysis of the data points using Prism software (v. 6.00, GraphPad Software Inc.)

	Resulting concentration Tetrazine [mM]	Initial concentration sTCO [mM]	Resulting concentration sTCO [mM]	k_{obs}	k_2 [$M^{-1}s^{-1}$]	Mean k_2 [$M^{-1}s^{-1}$]
syn-sTCO	0.05	0.49	0.245	8.415	34347	36,100 +/− 1,400
		0.98	0.49	18.41	37571	
		1.96	0.98	35.08	35796	
		2.94	1.47	54.18	36857	
anti-sTCO		0.5	0.25	7.458	29832	31,700 +/− 1,300
		1.0	0.5	15.84	31680	
		2.0	1	32.51	32510	
		3.0	1.5	48.98	32653	

Table 1.3: Rate constants for the reaction of *trans*-cyclooctenes (sTCO's ***syn*** & ***anti***) with PEGylated tetrazine **6** at 25 °C in water : methanol (45:55) measured under pseudo first order conditions using SX 18MV-R stopped-flow spectrophotometer. Values were determined from an average of four runs.

REFERENCES

1) Sorensen, J. *Theranostics* **2012**, *2*, 427-36.

2) Schlyer D. J. *Ann. Acad. Med. Signapore* **2004**, *33*, 146-54.

3) Som, P.; Atkins, H. L.; Bandoypadhyay,D.; Fowler, J. S.; MacGregor, A. R., Matsui, K.; Oster, Z. H.; Sacker, D. F.; Shlue, C. Y.; Turner, H.; Wan, C. N.; Wolf, A. P.; Zabinski, S. V. *J. Nucl. Med.* **1980**, *21*, 670-75.

4) Zhu, A.; Lee, D.; Shim, H. *Semi. Oncol.* **2011**, *38*, 55-69.

5) Kolb, H. C.; Finn, M. G.; Sharpless, K. B. *Angew. Chem. Int. Ed.* **2001,** *40*, 2004-2021.

6) Marik, J.; Sutcliffe, J. L. *Tetrahedron Lett.* **2006**, *47*, 6681-6684.

7) Wang, M.; Svatunek, D.; Rohlfing, K.; Liu, Y.; Wang, H.; Giglio, B.; Yuan, H.; Wu, Z.; Li. Z.; Fox, J. M. *Theranostics* **2016**, *6*, 887-895.

8) Royzen, M.; Yap, G. P.; Fox, J. M. *J. Am. Chem. Soc.* **2008**, *130*, 3760-3761.

9) Blackman, M. L.; Royzen, M.; Fox, J. M. *J. Am. Chem. Soc.* **2008**, *130*, 13518-13519.

10) Selvaraj, R.; Fox, J. M. *Curr. Opin. Chem. Biol.* **2013**, *17*, 753-760.

11) Murrey, H. E.; Judkins, J. C.; Am Ende, C. W.; Ballard, T. E.; Fang, Y.; Riccard, K.; Di, L.; Guilmette, E. R.; Schwartz, J. W.; Fox, J. M.; Johnson, D. S. *J. Am. Chem. Soc.* **2015**, *137*, 11461-11475.

12) Liu, S.; Zhang, H; Remy R. A.; Deng, F.; Mackay, M. E.; Fox, J. M.; Jia, X. *Adv. Mater.* **2015**, *27*, 2783-27890.

13) Wu, Z.; Liu, S.; Hassink, M.; Nair, I.; Park, R.; Li, L.; *et. al*. *J. Nuc. Med.* **2013**, *54*, 244-251.

14) Liu, S.; Hassink, M.; Selvaraj, R.; Yap, L-P.; Park, R.; Wang, H.; *et al*. *Molecular Imaging* **2013**, *12*, 121-128.

15) Selvaraj, R.; Liu, S.; Hassink, M.; Huang, C-W.; Yap, L-P.; Park, R.; *et al*. *Bioorg Med. Chem. Lett.* **2011**, *21*, 5011-5014.

16) Selvaraj, R.; Giglio, B. C.; Liu, S.; Wang, H.; Wang, M.; Yuan, H.; *et al*. *Bioconjug. Chem.* **2015**, *26*, 435-442.

17) Wyffels, L.; Thomae, D.; Waldron, A. M.; Fissers, J.; Dedeurwaerdere, S.; Van der Veken, P.; *et. al. Nucl. Med. Biol.* **2014**, *41*, 513-523.

18) Darko, A.; Wallace, S.; Dmitrenko, O.; Machovina, M. M.; Mehl, R. A.; Chin, J. W.; *et al*. *Chem. Sci.* **2014**, *5*, 3770-3776.

19) Taylor, M. T.; Blackman, M. L; Dmitrenko, O.; Fox, J. M. *J. Am. Chem.Soc.* **2011**, *133*, 9646-9649.

20) Zhang, H.; Dicker, K. T.; Xu, X.; Jia, X.; Fox, J. M. *ACS Macro Lett.* **2014**, *3*, 727-731.

21) Haubner, R.; Kuhnast, B.; Mang, C.; Weber, W. A.; Kessler, H.; Wester, H.; Schwaiger, M. *Bioconjug. Chem.* **2004**, *15*, 61-69.

22) Li, Z. B.; Wu, Z.; Chen, K.; Chin, F. T.; Chen, X. *Bioconjug. Chem.* **2007**, *18*, 1987-1994.

23) Wu, Z.; Li, Z. B.; Cai, W.; He, L.; Chin, F. T.; Li, F.; Chen, X. *Eur. J. Nucl. Med. Mol. Imaging* **2007**, *34*, 1823-1831.

24) Wu, Z.; Li, Z. B.; Chen, K.; Cai, W.; He, L.; Chin, F. T.; Li, F.; Chen, X. *J. Nucl. Med.* **2007**, *48*, 1536-1544.

25) Giancotti, F. G.; Ruoslahti, E. *Science* **1999**, *285*. 1028-1032.

26) Panne, P.; Fox, J. M. *J. Am. Chem. Soc.* **2007**, *129*, 22-23.

27) Hassink, M. D. PhD. Dissertation, University of Delaware, 2012.

Chapter 2

SYNTHESIS AND QUANTIFICATION OF TETRAZINE-ANTIBODY CONJUGATES

2.1 Introduction

A difficulty associated with the imaging of radiolabeled substrates is the ability to capture high resolution of tumors due to a necessary concentration within cancerous cells as opposed to uptake in surrounding normal tissues.[2] In therapy, difficulties arise when selectively delivering the therapeutic agent to the tumor while sparing normal tissues from toxicities in the process.[2] To solve these complications, radiolabeled peptides and proteins have been analyzed over a number of years.

Initially, the evaluation of tumor detection by single-photon imaging was studied through radiolabeled antibodies, however due to the evolution of FDG PET imaging; these developments began to subside.[1] While the use of FDG has made quite an impact on tumor diagnosis and analysis, the need for improved resolution and lack of specificity for different types of cancers enabled further study into additional biomolecules. Through the improvement of radiolabeled techniques, antibodies in particular have become of interest for radioimmunodetection and radioimmunotherapy applications.[2]

A primary antibody used for radiolabeling applications is IgG, a large protein with a molecular weight of ~150 kD.[2] Due to the large size associated with IgG, clearance from the blood is elongated, requiring multiple days (1 – 3) before a critical

amount is consumed within a tumor for efficient detected radioactivity.[2, 3] Molecular engineering has provided the delivering of antibodies as reduced fragments allowing sufficiently increased blood clearance as well as improved tumor uptake.[2] While this advancement did provide benefits, it also contains a caveat of having reduced amounts of the radiolabeled antibody reaching the tumor with shorter residence times.[2, 4, 5]

One specific strategy that has innovated the use of antibodies for these applications is pretargeting imaging and therapy. This approach separates the antibody targeting moiety from the radiolabeled molecule, administering the radionuclide only after optimal pretargeting by the antibody has occurred.[2] This targeting was first achieved using a bispecific antibody (bsMAb) that binds to an antigen.[6, 7] Additional pretargeting studies in small animals has shown that tumor consumption of radionuclides is consistent with those of directly labeled IgG, however, the same tumor uptake occurs within minutes as opposed to days.[8] More importantly, the radionuclide is cleared very rapidly within a few hours and the tumor : blood tissue ratio is > 10:1 after 1 hour post injection.[2, 9]

Over the years, several pretargeting methods have evolved, not only benefiting the radioimaging of tumors, but also advancing antibody use in therapeutic applications. Studies have shown that antibodies used at high doses in combination with chemotherapy have displayed high response rates in the treatment of lymphoma.[1, 10] The development of therapeutic approaches using antibodies has also become of interest for many pharmaceutical companies. Due to the results observed from the modified RGDyK peptide conjugate (**^{18}F-8**) described in Chapter 1, it was of interest to apply this system to larger proteins such as antibodies. With the improved tumor uptake and blood circulation of our F-18 probe relative to other peptide conjugates and the benefits of

imaging and therapy offered with antibodies, it is appealing to combine these two models for *in vivo* pretargeting PET studies.

2.2 Results and Discussion

For this work, diphenyl-*s*-tetrazine in addition to other tetrazines were studied for antibody modification and methods were developed in order to quantify the degree of labeling. The synthetic work for this project was completed by Dr. Raghu Vannam, a postdoctoral researcher within the Fox lab. Each of these tetrazines could be developed in a few steps starting from commercially available reagents. Methods to prepare diol-tetrazine (**9**) were initially developed by He Zhang and completed by Raghu. To improve the water stability and pharmokinetic properties, PEGylated chains were incorporated during the synthetic procedures to receive tetrazines **6a**, **9** and **10** (**Figure 2.1**).

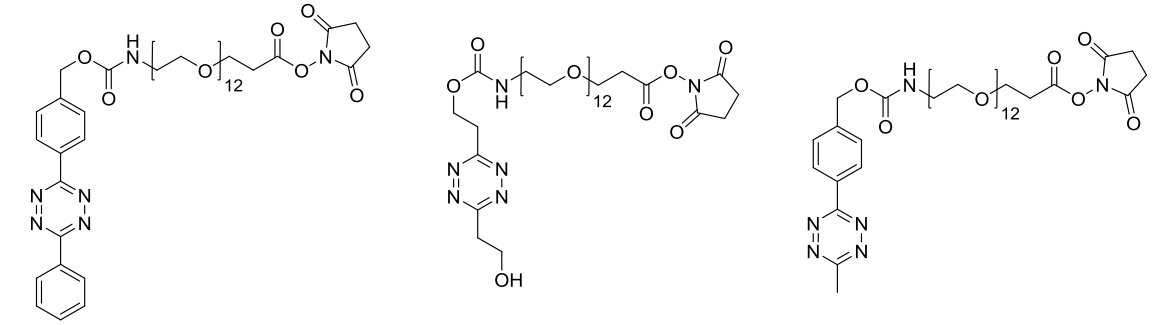

Figure 2.1: Tetrazines used for antibody conjugation.

Each of these tetrazines were then conjugated with antibody (TNT or IgG) and various methods were developed in order to quantify the degree of labeling. For this

project, the aim was to add varying stoichiometric amounts of tetrazine in order to modify antibody with about two tetrazines. Achieving a degree of labeling of about two would allow a suitable amount of tetrazine present for ^{18}F-sTCO conjugation for radiolabeling imaging and therapy applications. Secondly, this also avoids over modifying the antibody with tetrazine which could cause precipitation out of an aqueous solution as well as possible defunctionalization of the antibody.

The first method developed in order to quantify the degree of labeling was by measuring exact mass of modified samples via MALDI-TOF. However, due to the large molecular weight associated with antibodies as well as the presence of tetrazine, these samples were unable to be ionized from the sample plate and measured by mass. A second method was developed where measurements were obtained via Nanodrop UV-Vis Spectrophotometer. During this process, samples were prepared using 20 μM of antibody and then modified with stoichiometric amounts of tetrazine (1:1 – 4:1, 20 μM – 80 μM) in 1xPBS at pH = 7.4. While using this protocol, data could only be recorded for the diphenyl-Tz NHS **6a** since the maximum absorbance by UV-Vis (300 nm) did not overlap with the antibody maximum absorbance (280 nm) (**Figure 2.2**).

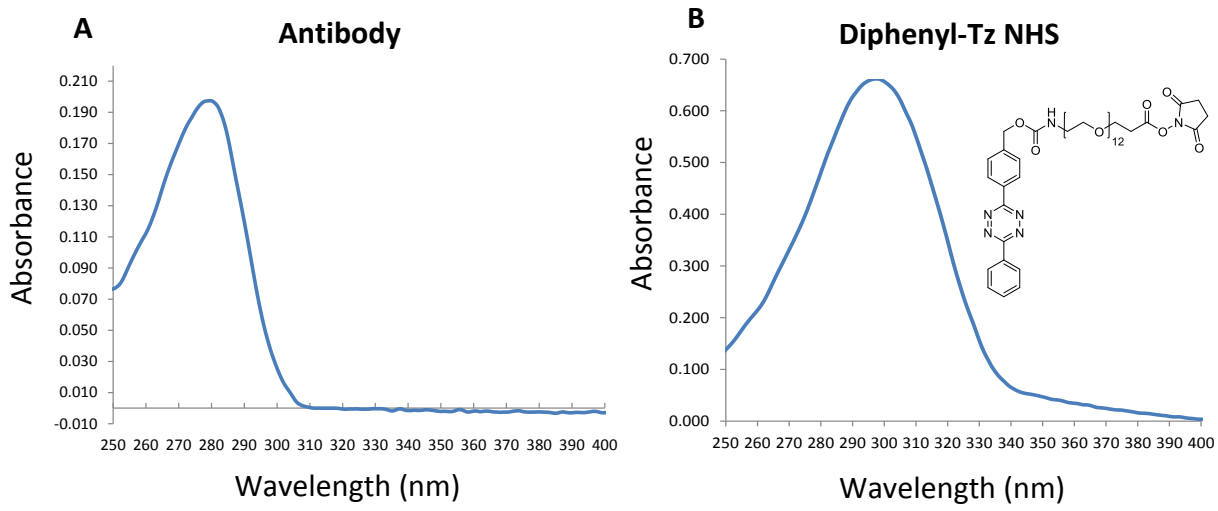

Figure 2.2: UV-Vis absorbance spectra in 1xPBS at pH = 7.4 of (**A**) antibody with maximum absorbance of 300 nm and (**B**) diphenyl-*s*-tetrazine **6a** with maximum absorbance of 280 nm.

After sitting at room temperature for 1 h, UV-Vis measurements were obtained for crude samples which were then purified by microdialysis. During this process, only small amounts of antibody samples were prepared (5 – 10 μL), so even the smallest commercially available dialysis tubing would not be suitable during purification due to intended loss of material and extreme dilution of modified samples. For purification, devices were prepared with the assistance of Dr. Colin Thorpe, a Professor of Chemistry and Biochemistry at the University of Delaware (**Figure 2.3**). A 50 mL centrifuge tube was cut near the top and dialysis tubing with a 10,000 molecular weight cut-off was secured beneath the lid (**Figure 2.3A**). For demonstration, a 5 μL sample of concentrated blue dye was spotted on the dialysis tubing (**Figure 2.3B**) and placed in a 250 mL beaker containing 1xPBS at pH = 7.4 (**Figure 2.3C**). A control experiment was also conducted where tetrazine **6a** (20 μM) was subjected to dialysis overnight using the

set-up as shown and UV-Vis measurements were obtained before and after purification. The data showed that after purification, tetrazine could no longer be observed in the absorbance spectrum. This experiment demonstrated that any unbound tetrazine in the modified antibody samples would sufficiently pass through the dialysis membrane during purification in order to quantify accurate degree of labeling.

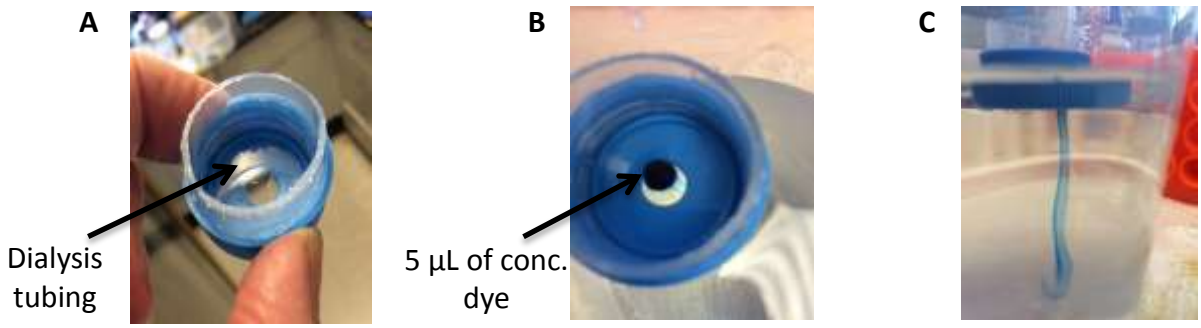

Figure 2.3: Microdialysis apparatus prepared for purification of modified antibody samples. (**A**) 50 mL centrifuge tube cut with dialysis membrane secured in the lid. (**B**) Sample of concentrated dye spotted on dialysis tubing. (**C**) Demonstration of dialysis of concentrated dye in a 250 mL beaker containing 1xPBS at pH = 7.4.

Modified antibody samples were subjected to dialysis overnight at 4 °C and then UV-Vis measurements were obtained (**Figure 2.4**). Measurements were obtained by determining the absorbance at 310 nm and 280 nm and dividing these values to receive a ratio. The ratio for the purified sample was then compared to the crude ratio in order to evaluate the degree of labeling. For example, a 10 µL sample of antibody (20 µM) modified with two equivalents of tetrazine **6a** (40 µM), the degree of labeling observed ranged in values from 0.86 – 1.2. It was also detected for these samples, if five

equivalents of tetrazine (100 μM) or more were added; the modified antibody became too hydrophobic and precipitated out of solution.

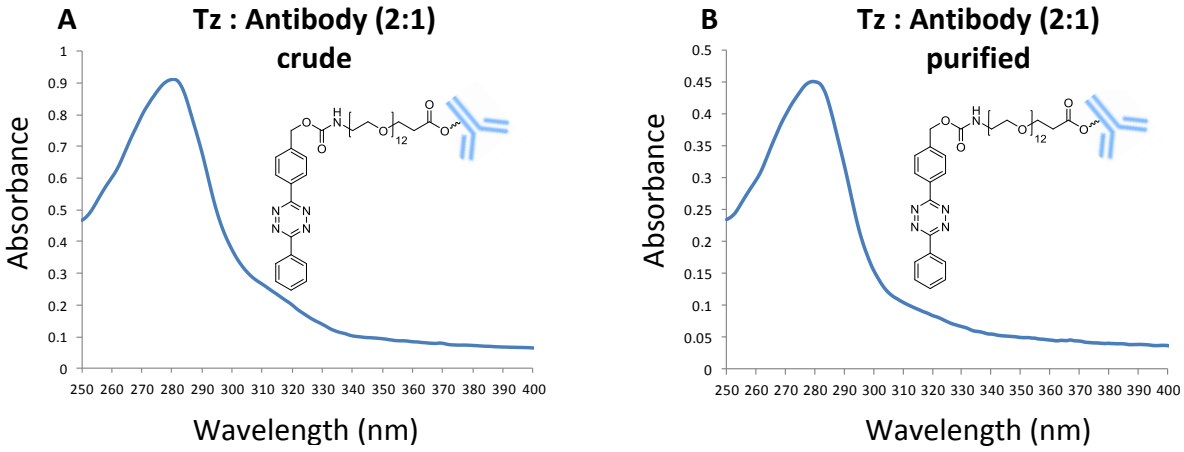

Figure 2.4: UV-Vis spectra of modified antibody samples. (**A**) Crude spectra of antibody measured with two equivalents of tetrazine **6a**. (**B**) Purified spectra of antibody measured with two equivalents of tetrazine **6a**.

While UV-Vis data could be obtained for the diphenyl-*s*-tetrazine **6a**, this method was not suitable for diol-Tz **9** or Me-phenyl-Tz **10** due to an overlap in maximum absorbance between the antibody and corresponding tetrazine. In order to assess the degree of labeling for the remaining tetrazines, a gel assay was developed and measured via fluorescence using an image processing program, ImageJ. For this assay, samples of antibody (TNT or IgG, 30 μM) were modified with stoichiometric amounts of the respective tetrazine (1:1 – 20:1, 30 μM – 600 μM) in 1xPBS at pH = 7.4. For the diphenyl-Tz **6a**, modifying antibody with four equivalents could be achieved while maintaining a homogenous solution. For less hydrophobic tetrazines **9** and **10**, twenty

equivalents of tetrazine could be added to antibody without experiencing any precipitation. Modified antibody samples were then reacted with 1.5 equivalents (45 – 900 μM) of sTCO containing a fluorophore (Alexa-647) for 10 min. at 25 °C (**Scheme 2.1**).[11] Various dyes were analyzed including Alexa-Fl, BODIPY-Fl and TAMRA-Fl. Of these fluorescent molecules, Alexa-Fl was chosen due to its adequate solubility in aqueous mediums necessary for these studies. Using BODIPY-Fl or TAMRA-Fl which weren't as water soluble would cause the tetrazine-antibody conjugates to precipitate out of solution.

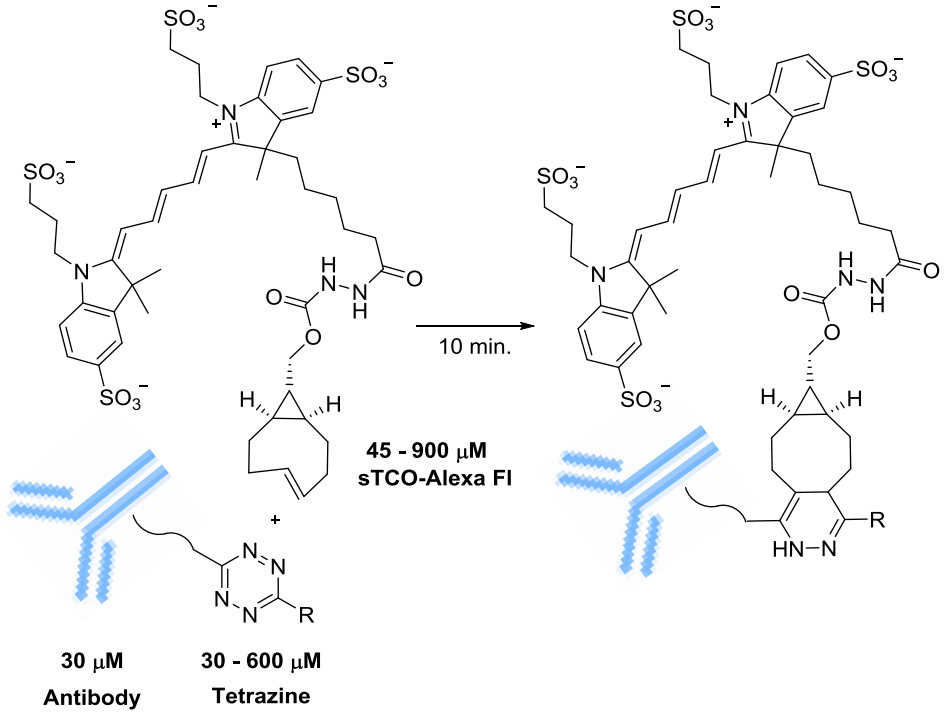

Scheme 2.1: Reaction of tetrazine-antibody construct with Alexa 647-sTCO.[11]

Samples were then loaded onto an SDS reducing page gel. As observed in **Figure 2.5**, the antibody is reduced into heavy and light chains, with the higher molecular weight bands lying near the top of the gel and the lower bands settling near the bottom. For less hydrophilic tetrazines (**6a**) antibody samples were evaluated by in-gel fluorescence for modifications of up to 4 equivalents of tetrazine (**Figure 2.5A**). For more water soluble tetrazines (**9** & **10**), antibody samples were analyzed containing modifications of up to 20 equivalents (**Figure 2.5B** & **2.5C**).

Imaging of the gels and analysis shows that as the amount of tetrazine conjugated to antibody increases, the bands begin to shift upwards indicating an increase in molecular weight. The intensity in fluorescence measured through the sTCO-Alexa-Fl also increases where higher amounts of tetrazine are present, with the 4:1 and 20:1 modified samples displaying the brightest bands on the gel. Comparatively, diphenyl-tetrazine (**6a**) showed the brightest fluorescence and highest modification of the imaged gels for the stoichiometric amounts of tetrazine reacted to antibody. Diol-tetrazine displayed significantly lower fluorescence in relation to tetrazines **6a** and **10**.

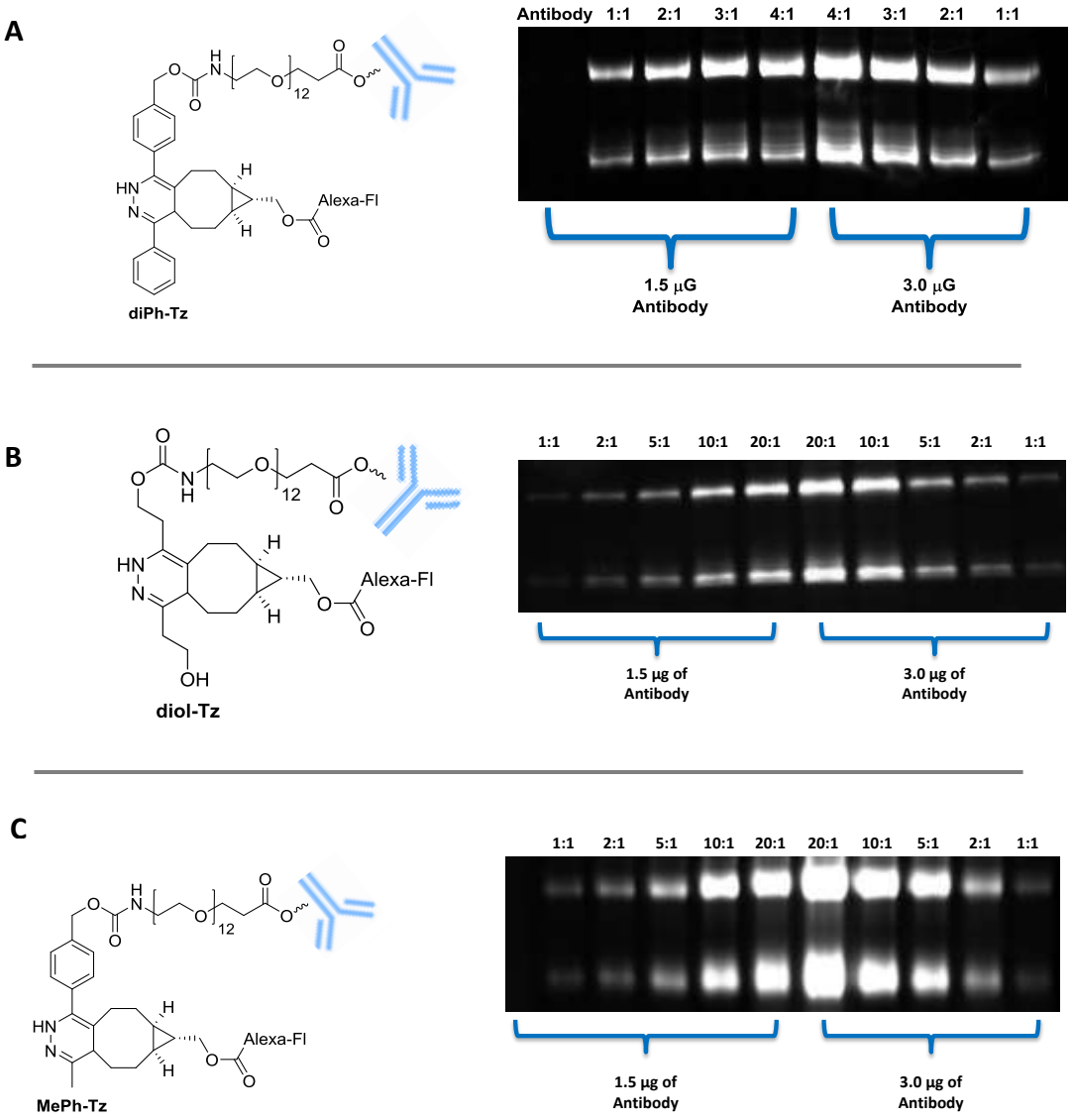

Figure 2.5: Gel imaging assay for quantification of tetrazine-antibody conjugates and measurement through fluorescence of sTCO-Alexa-Fl. (**A**) Gel image of antibody modified with stoichiometric amounts of diphenyl-tetrazine (**6a**). (**B**) Gel image of antibody modified with stoichiometric amounts of diol-tetrazine (**9**). (**C**) Gel image of antibody measured with stoichiometric amounts of methyl-phenyl-tetrazine (**10**).

In order to quantify the degree of labeling, a standard containing exactly one tetrazine was prepared by conjugating methyl-phenyl-tetrazine maleimide to a wild-type of thioredoxin reductase through a cysteine residue (**Scheme 2.2**).

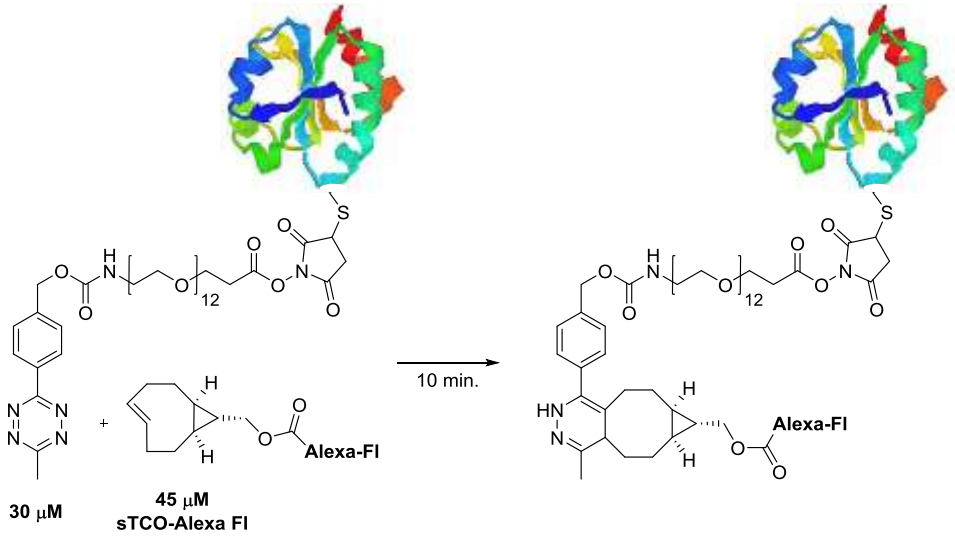

Scheme 2.2: Thioredoxin reductase modified with Me-Ph-Tz maleimide and reacted with 1.5 equivalents of sTCO-Alexa Fl in 1xPBS at pH = 7.4. At room temperature, the reaction is complete within 10 min.

The gel images were then analyzed via ImageJ and fluorescence of the tetrazine-antibody modified samples were compared to the standard (**Figure 2.6**). For diphenyl-tetrazine (**6a**), stoichiometric amounts of 1:1, 2:1, 3:1 and 4:1 tetrazine : antibody resulted in corresponding degrees of labeling of 0.67, 0.90, 1.2 and 2.1 respectively (**Figure 2.6A**). Stoichiometric amounts of 1:1, 2:1, 5:1, 10:1 and 20:1 tetrazine : antibody for tetrazine **10** resulted in corresponding degrees of labeling of 0.43, 0.74, 2.2, 4.0 and 7.5 (**Figure 2.6B**).

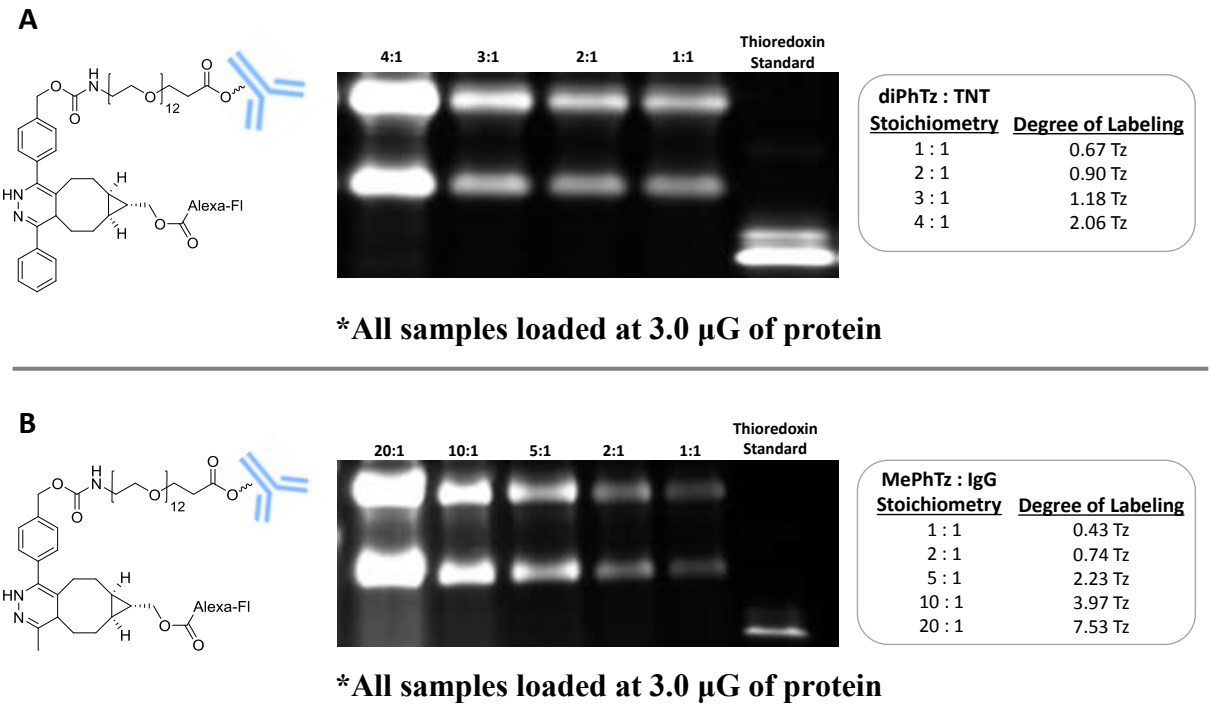

Figure 2.6: Gel images of tetrazine : antibody samples compared to fluorescently labeled thioredoxin standard. (**A**) Gel image of tetrazine **6a** with calculated degrees of labeling. (**B**) Gel image of tetrazine **10** with calculated degrees of labeling.

To estimate the degree of labeling for diol-tetrazine (**9**), the data was calibrated based on the results obtained for the fluorescence measured and degree of labeling calculated for tetrazine **6a**. As shown in **Figure 2.7**, a sample of antibody reacted with two equivalents of tetrazine **6a** displays significantly higher fluorescence in comparison to a 2:1 sample of antibody modified with diol-tetrazine (**9**).

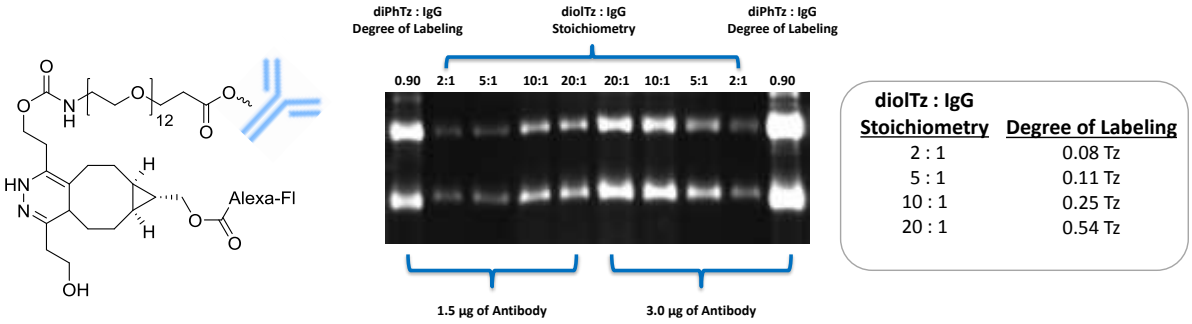

Figure 2.7: Degrees of labeling calculated for antibody samples modified with diol-tetrazine (**9**). Data estimated based on fluorescence measured and degree of labeling calculated for tetrazine **6a**.

For samples of tetrazine **9** reacted with antibody, the measured fluorescence was compared to antibody conjugates of diphenyl-tetrazine (**6a**) where the degree of labeling had been measured to be 0.90. Based on this degree of labeling, it was found that stoichiometric amounts of 2:1, 5:1, 10:1 and 20:1 diol-tetrazine : antibody concluded in estimated degrees of labeling of 0.08, 0.11, 0.25 and 0.54.

2.3 Conclusions

The tetrazine ligation as an ^{18}F-probe for radiolabeling imaging applications previously discussed in Chapter 1 exhibited increased blood circulation and tumor uptake relative to other cyclic RGDyK peptide systems. Due to these results, it was of interest to expand this system to larger proteins and antibodies for additional use in radio-imaging applications. Different methods were explored in order to assess an accurate degree of labeling based on the stoichiometric amount of tetrazine reacted with antibody (TNT or IgG). Various approaches were investigated including the measurement of exact mass through MALDI-TOF, analysis of absorbance via Nanodrop UV-Vis Spectrophotometer as well as the evaluation of fluorescence using a

reducing page gel imaging assay. Of these three approaches, quantifying degree of labeling by in-gel fluorescence was shown to be the most suitable method for the various types of tetrazines analyzed.

The different types of tetrazine reacted with samples of antibody included diphenyl-Tz (**6a**) and more water soluble tetrazines such as diol-tetrazine (**9**) and methyl-phenyl Tz (**10**). For the more hydrophilic substrates (**9** & **10**), modifications using up to 20 equivalents of tetrazine could be added while maintaining a homogeneous solution. For the less water stable derivative (**6a**), only 4 equivalents of tetrazine could be added. Going above 5 equivalents of substrate resulted in precipitation of the antibody conjugate from the aqueous medium. After tetrazine-antibody conjugates were prepared, an excess of sTCO-Alexa Fl was added to each sample and loaded onto a SDS-page gel.

In order to measure fluorescence, images of the gels were obtained and the light and heavy chains were analyzed via ImageJ. To quantify the degree of labeling, a standard containing thioredoxin conjugated with exactly one tetrazine was reacted with sTCO-Alexa-Fl and the fluorescence was measured to be used as a comparison for the tetrazine-antibody conjugates. Based on this comparison, it was observed that antibody samples modified with 1:1, 2:1, 3:1 and 4:1 equivalents of tetrazine (**6a**) resulted in values of about 0.67, 0.90, 1.2 and 2.1 for the corresponding degree of labeling. A degree of labeling measured through in-gel fluorescence for a 2:1 sample was also comparative to calculated values of 0.86 – 1.2 obtained via UV-Vis absorbance measurements for tetrazine **6a**. Samples of antibody modified with 1:1, 2:1, 5:1, 10:1 and 20:1 equivalents of tetrazine **10** resulted in degrees of labeling of 0.43, 0.74, 2.2, 4.0 and 7.5. Diol-tetrazine (**9**) displayed considerably lower degrees of labeling of 0.08,

0.11, 0.25, and 0.54 for antibody samples modified with 2:1, 5:1, 10:1 and 20:1 equivalents of substrate.

Comparatively, diphenyl-tetrazine displayed the highest degrees of labeling relative to the stoichiometric amounts of substrate reacted with antibody. Diol-tetrazine displayed the lowest degrees of labeling which can be observed in the fluorescence emitted in the gel images as well as the values estimated. While the gel images and analysis of the data conclude that it is possible to modify antibody with high levels of tetrazine, more modest amounts will be used for future applications. In order to prevent defunctionalization of antibody or possible precipitation out of solution, it will be desirable to conjugate antibodies with stoichiometric amounts of tetrazine that correspond to a degree of labeling of about 2.0.

REFERENCES

1) Barbet, J.; Bardies, M.; Bourgeois, M.; Chatal, J.; Cherel, M.; Davodeau, F.; *et. al. Methods in Molecular Biology*, **2012**, *907*, 681.

2) Goldenberg, D. M.; Chatal, J.; Barbet, J.; Boerman, O.; Sharkey, R. M. *Update Cancer Ther.* **2007**, *2*, 19.

3) Buchsbaum, D. J. *Cancer Res.***1995**, *55*, 5729.

4) Sharkey, R. M.; Motta, C.; Pawlyk, D.; Siegel, J. A.; Goldenberg, D. M.; *Cancer Res*. **1990**, *50*, 2330.

5) Behr, T. M.; Sgouros, G.; Stabin, M. G.; *et al. Clin. Cancer Res.* **1999**, *5*, 3031.

6) Goodwin D, A; Meares, C. F.; David, G. F. *et al. Int. J. Rad. Appl. Instrum. B.* **1986**, *13*, 383.

7) Reardan, D. T.; Meares, C. F.; Goodwin, D. A.; *et al. Nature*, **1985**, *316*, 265.

8) Sharkey, R. M.; Karacay, H.; Cardillo, T.M.; *et al. Clin. Cancer Res.* **2005**, *11*, 7109.

9) Axworthy, D. B.; Reno, J. M.; Hylarides, M. D.; *et al. Proc. Natl. Acad. Sci.* **2009**, *97*, 1802.

10) Dillman, R. O. *Cancer Biother. Radiopharm.* **2011**, *26*, 1.

11) Zhang, H.; Dicker, K. T.; Xu, X.; Jia, X.; Fox, J. M. *ACS Macro Lett.* **2014**, *3*, 727-731.

Chapter 3

DEVELOPMENT OF SILVER NITRATE COMPLEXES TO ENHANCE THE SHELF-LIFE OF F-18 LABELING PRECURSORS

3.1 Introduction

In recent work within the Fox lab, an organelle-targetable model system was developed in order to assess the reactivity, specificity and stability of bioorthogonal reagents in live cells.[1] To evaluate this model, two bioorthogonal chemistries were explored including, the strain promoted azide-alkyne cycloaddition (SPAAC) between cyclooctynes and azides as well as the Inverse electron-demand Diels−Alder (IEDDA) reaction of strained cycloalkenes and cyclooctynes with tetrazines.[2–5] A HaloTag fusion protein was selected and these properties were analyzed via fluorescence through the direct incorporation of fluorophore constructs.[1]

For this application, it was found that the reaction between strained *trans*-cyclooctene (sTCO) and monosubstituted tetrazines is the fastest occurring system;[1] sTCO compounds are stable in solution and are effective reagents for cell-based labeling studies. However, the shelf-life of sTCO compounds is modest, and for long-term storage sTCO compounds should be kept in cold solution.[7, 8] In practice, this led to variable results in cell labeling studies with stock solutions that were more than one week old. To assess the stability of sTCO derivatives, Yinshi Fang heated neat sTCO at 30 ^{o}C for 3 days (**Scheme 3.1**)[1] It was observed that almost complete decomposition occurred with a trace amount of the *cis*-isomer present.

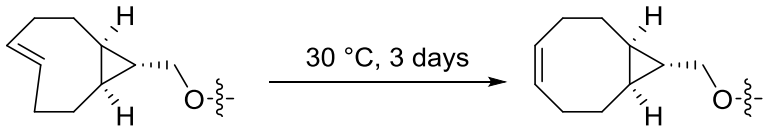

sTCO

Scheme 3.1: Degradation and some *trans*-*cis* isomerization of sTCO following a 3-day incubation neat at 30 °C.

During preparation of sTCO, the *cis*-cyclooctene is photoisomerzied in a flow reactor where the *trans*-isomer is isolated through selective complexation with $AgNO_3$-infused silica gel.[9, 10] The sTCO is then liberated when the silica gel is stirred in aqueous NH_4OH. For this work, it was hypothesized that preparing these sTCO substrates as their silver complexes would provide long-term stability for storage, yet be applied directly to a cell culture where high concentrations of NaCl would release the reactive sTCO. To assess the stability, Ag-sTCO substrate was prepared and incubated neat at 30 °C for 3 days. Evaluation showed that in comparison to the silver free complex, improved stability with no degradation of reagent or *trans*-to-*cis* isomerization was exhibited (**Scheme 3.2**).[1]

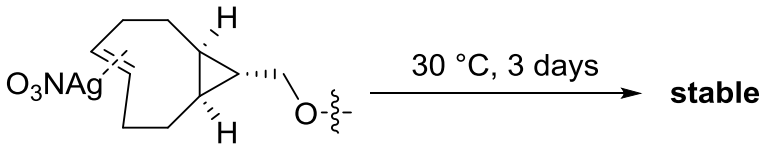

Ag-sTCO

Scheme 3.2: No degradation or *trans*-to-*cis* isomerization of sTCO following a 3-day incubation neat at 30 °C.

Two substrates commonly synthesized in the Fox lab include radiolabeled precursors sTCO-tosylate and TCO-nosylate (**Figure 3.1**).[11, 12] These reagents previously discussed in Chapter 1 have both been used for ^{18}F-PET imaging studies within tumor bearing mice. Problems occur when preparing these derivatives which include *trans*-to-*cis* isomerization during synthesis or instability while storing for long periods of time. Due to the improved stability exhibited with Ag-sTCO HaloTag ligands in recent work[1], it was desirable to apply this chemistry to F-18 radiolabeling precursors for enhanced shelf-life.

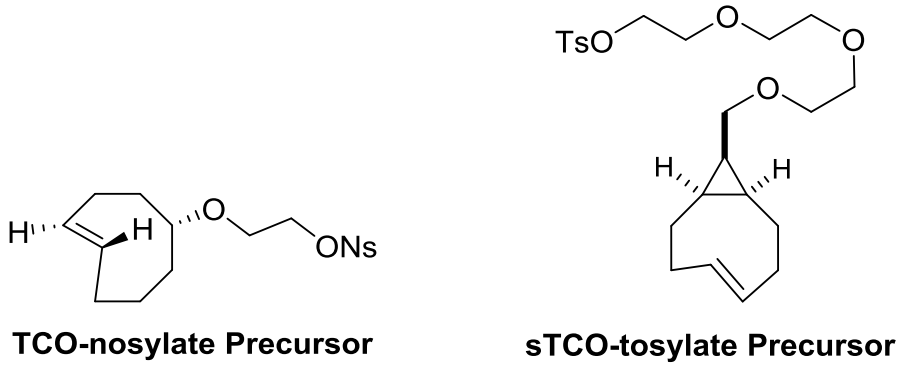

Figure 3.1: F-18 labeling precursors synthesized for use in PET imaging studies.[11-13]

3.2 Results and Discussion

The TCO-Ns precursor is relatively more stable in comparison to sTCO; however problems occur in synthesis when converting TCO-alcohol **11**[13] to the nosylate precursor. During this step, *trans*-to-*cis* isomerization occurs in quantities sometimes as high as 30%, even when using a freshly opened bottle of *p*-nitrosulfonyl chloride (**Scheme 3.3**).

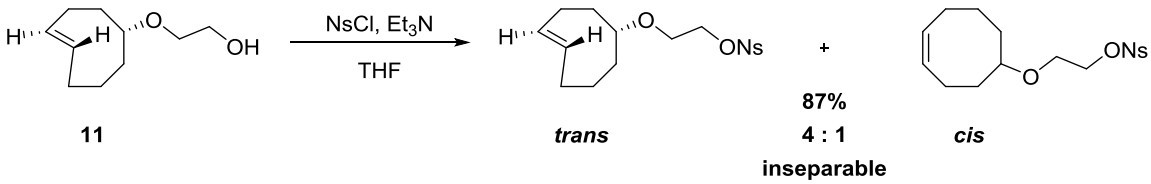

Scheme 3.3: *trans*-to-*cis* isomerization during conversion of alcohol **11**[13] to the nosylate precursor.

Initial efforts to transform *cis*-nosylate complex **12** to the *trans*-substrate by flow photoisomerization chemistry (**Scheme 3.4A**) resulted in low conversion rates over long reaction times (only ~10% after 18 h). Additional methods were explored where the 4:1 inseparable mixture was pumped over a bed of $AgNO_3$-embedded silica gel (**Scheme 3.4B**). The affinity for the *trans*-reagent to more effectively bind to silver while the *cis*-cyclooctene elutes off the column resulted in complete separation of these isomers. TCO-nosylate **13** can then be recovered in 67% yield upon stirring the silica gel with aqueous NH_4OH.

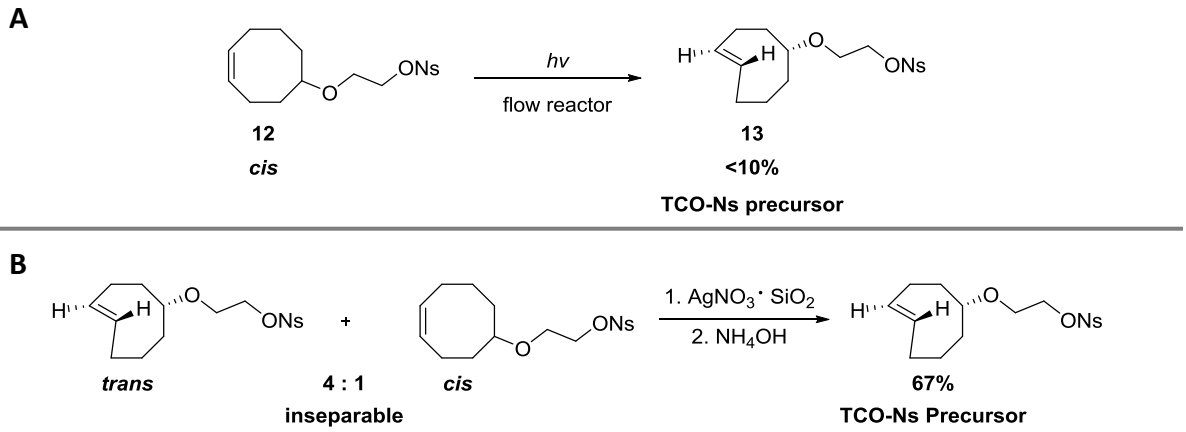

Scheme 3.4: (**A**) Photoisomerization of *cis*-nosylate **12**. (**B**) Separation of *trans* and *cis* isomers via silver-ion chromatography.

The silver nitrate complex of sTCO labeling precursor **3** was prepared to enhance long-term storage for this reagent. When stored neat or in various solvents (MeOH, THF, CH_3CN) at -15°C, isomerization or degradation of product occurs at intermediate storage times (< 1 month). To increase the shelf-life, Ag-sTCO tosylate **14** was prepared in quantitative yields by simply stirring the sTCO substrate in anhydrous methanol with 1.1 equivalents of $AgNO_3$ at r.t. for 1 hour (**Scheme 3.5**) Observation by ^1H NMR in deuterated methanol after being stored neat at -15 °C for 45 days showed no isomerization or degradation of product. The reactive sTCO could be liberated by stirring with aq. NH_4OH and retrieved upon extraction with an organic solvent. Work-up methods involving NH_4Cl or NaCl resulted in an undesirable exchange of the tosylate group.

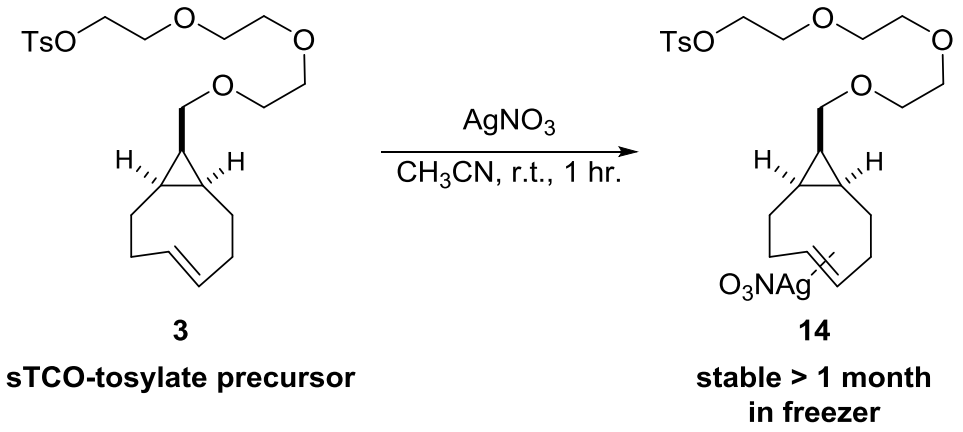

Scheme 3.5: Synthesis of Ag-sTCO tosylate for enhanced shelf-life.

3.3 Conclusions

Silver complexes of sTCO substrates have been shown to have improved stability for applications and storage over long periods of time. Due to stability issues during preparation and storage of F-18 labeling precursors frequently synthesized in the Fox lab, it was of interest to apply this chemistry to these reagents. During conversion of the TCO-alcohol to the nosylate substrate, *trans-cis* isomerization occurs in ~ 30% yields. Silver-ion chromatography can effectively be utilized to easily separate these isomers. Ag-sTCO tosylate was formed in order to enhance the shelf-life for this reagent. The silver free complex is stable for less than a month, even when stored at -15 ^{o}C in solvent. In comparison, Ag-sTCO tosylate is stable when stored neat at -15 ^{o}C for over a month, with no sign of isomerization or product decomposition.

3.4 Experimental Section

3.4.1 General Considerations

All reactions were carried out in glassware that was flame-dried under vacuum and cooled under nitrogen. All commercially available reagents and solvents were used as received. 2-(2-(2-((*syn*-(*E*)-bicyclo[6.1.0]non-4-en-9-yl)methoxy)ethoxy)ethoxy)ethyl 4-methylbenzenesulfonate and 2-[*rel*-(1R-4E-pR)-cyclooct-4-en-1-yloxy]ethyl 4-nitrobenzenesulfonate were prepared following known procedures.[11,13] Reactions were monitored by thin layer chromatography (TLC) performed on SiliCycle silica gel GF 250 μm plates and were visualized with ultraviolet (UV) light (254 nm) and/or $KMnO_4$ staining. Flash chromatography was performed using normal phase SiliCycle silica gel (40-63D, 60Å). ^{1}H, and ^{13}C nuclear magnetic resonance (NMR) chemical shifts are reported in ppm relative to MeOH (i.e. ^{1}H NMR δ = 3.31 and ^{13}C NMR = 49.1).

3.4.2 Synthetic Procedure

2-(2-(2-((*syn*-(*E*)-bicyclo[6.1.0]non-4-en-9-yl)methoxy)ethoxy)ethoxy)ethyl 4-methylbenzenesulfonate-$AgNO_3$ (14)

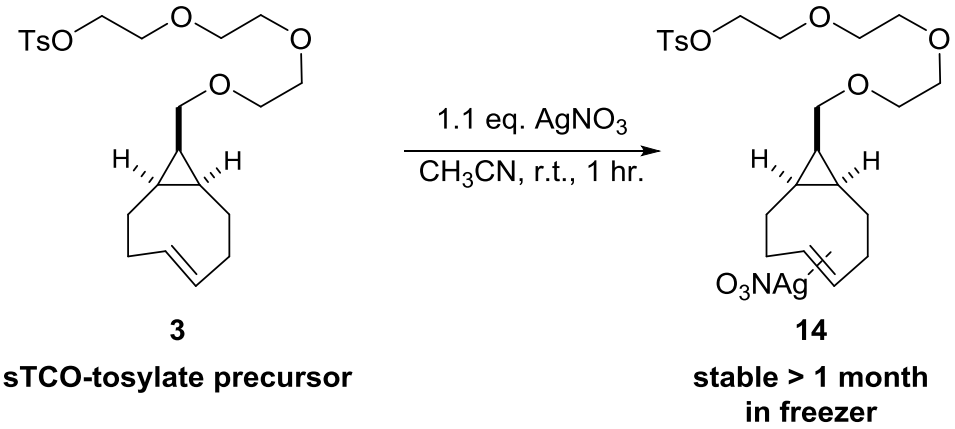

3
sTCO-tosylate precursor

14
stable > 1 month in freezer

Tosylate **3** (10 mg, 0.023 mmol) was added into a flame-dried round bottom flask containing anhydrous MeOH (0.5 mL, 0.04M) and silver nitrate (4.0 mg, 0.023 mmol). The mixture was stirred at room temperature for 1 h after which the solution was filtered through a plug of cotton and concentrated by rotatory evaporation to receive **14** in quantitative yields as an oil which was stored neat at -15 ^{o}C. ^{1}H NMR (600 MHz, CD_3OD) δ 7.80 (d, *J* = 8.0 Hz, 2H), 7.45 (d, *J* = 8.0 Hz, 2H), 6.06 (ddd, *J* = 16.5, 9.2, 6.0 Hz, 1H), 5.33 (ddd, *J* = 16.6, 10.6, 3.5 Hz, 1H), 4.18 – 4.10 (m, 2H), 3.68 – 3.64 (m, 2H), 3.61 – 3.53 (m, 8H), 3.47 (d, *J* = 7.7 Hz, 2H), 2.60 (dtd, *J* = 11.6, 4.0, 2.3 Hz, 1H), 2.46 (s, 3H), 2.31 – 2.19 (m, 3H), 2.17 – 2.12 (m, 1H), 1.98 – 1.90 (m, 2H), 1.39 – 1.31 (m, 1H), 1.29 – 1.16 (m, 1H), 1.05 (dtd, *J* = 14.8, 12.6, 2.3 Hz, 1H), 0.90 (dtd, *J* = 13.2, 8.8, 3.0 Hz, 1H), (small peaks attributable to impurities were detected by ^{1}H NMR at 3.35 and 1.40 ppm); ^{13}C NMR (151 MHz, MeOD) δ 146.48, 131.05, 129.02, 125.97, 118.68, 101.39, 71.67, 71.61, 71.50, 70.96, 70.95, 69.77, 68.48, 35.24, 34.57, 29.00, 28.25, 21.57, 19.91, 19.64, 18.13, (a small peak attributable to methanol was detected by ^{13}C at 49.9 ppm).

REFERENCES

1) Murrey, H. E.; Judkins, J. C.; Ende, C. W.; Ballard, E. T.; Fang, Y.; Riccardi, K.; Guilmette, E. R.; *et. al. J. Am. Chem. Soc.* **2015**, *137*, 11461.

2) Debets, M. F.; van Berkel, S. S.; Dommerholt, J.; Dirks, A. T.; Rutjes, F. P.; van Delft, F. L. *Acc. Chem. Res.* **2011**, *44*, 805.

3) Sletten, E. M.; Bertozzi, C. R. *Acc. Chem. Res.* **2011**, *44*, 666.

4) Selvaraj, R.; Fox, J. M. *Curr. Opin. Chem. Biol.* **2013**, *17*, 753.

5) Devaraj, N. K.; Weissleder, R. Acc. Chem. Res. 2011, 44, 816.

6) Seckute, J.; Devaraj, N. K. *Curr. Opin. Chem. Biol.* **2013**, *17*, 761.

7) Darko, A.; Wallace, S.; Dmitrenko, O.; Machovina, M. M.; Mehl, R. A.; Chin, J. W.; Fox, J. M. *Chemical Science* **2014**, *5*, 3770.

8) Taylor, M. T.; Blackman, M. L.; Dmitrenko, O.; Fox, J. M. *J. Am. Chem. Soc.* **2011**, *133*, 9646.

9) Taylor, M. T.; Blackman, M. L.; Dmitrenko, O.; Fox, J. M. *J. Am. Chem. Soc.* **2011**, *133*, 9646.

10) Royzen, M.; Yap, G. P.; Fox, J. M. *J. Am. Chem. Soc.* **2008**, *130*, 3760.

11) Wang, M.; Svatunek, D.; Rohlfing, K.; Liu, Y.; Wang, H.; Giglio, B.; Yuan, H.; Wu, Z.; Li. Z.; Fox, J. M. *Theranostics*, **2016**, *6*, 887.

12) Selvaraj, R.; Liu, S.; Hassink, M.; Huang, C-W.; Yap, L-P.; Park, R.; *et al*. *Bioorg Med. Chem. Lett.* **2011**, *21*, 5011-5014.

13) Selvaraj, R.; Giglio, B. C.; Liu, S.; Wang, H.; Wang, M.; Yuan, H.; *et al*. *Bioconjug. Chem.* **2015**, *26*, 435-442.

Appendix A

SPECTRAL DATA FOR CHAPTER 1

(rel-1R,8S,9S,4E)-Bicyclo[6.1.0]non-4-ene-9-ylmethanol (**2**)
^{1}H NMR (600 MHz, CD_3OD)

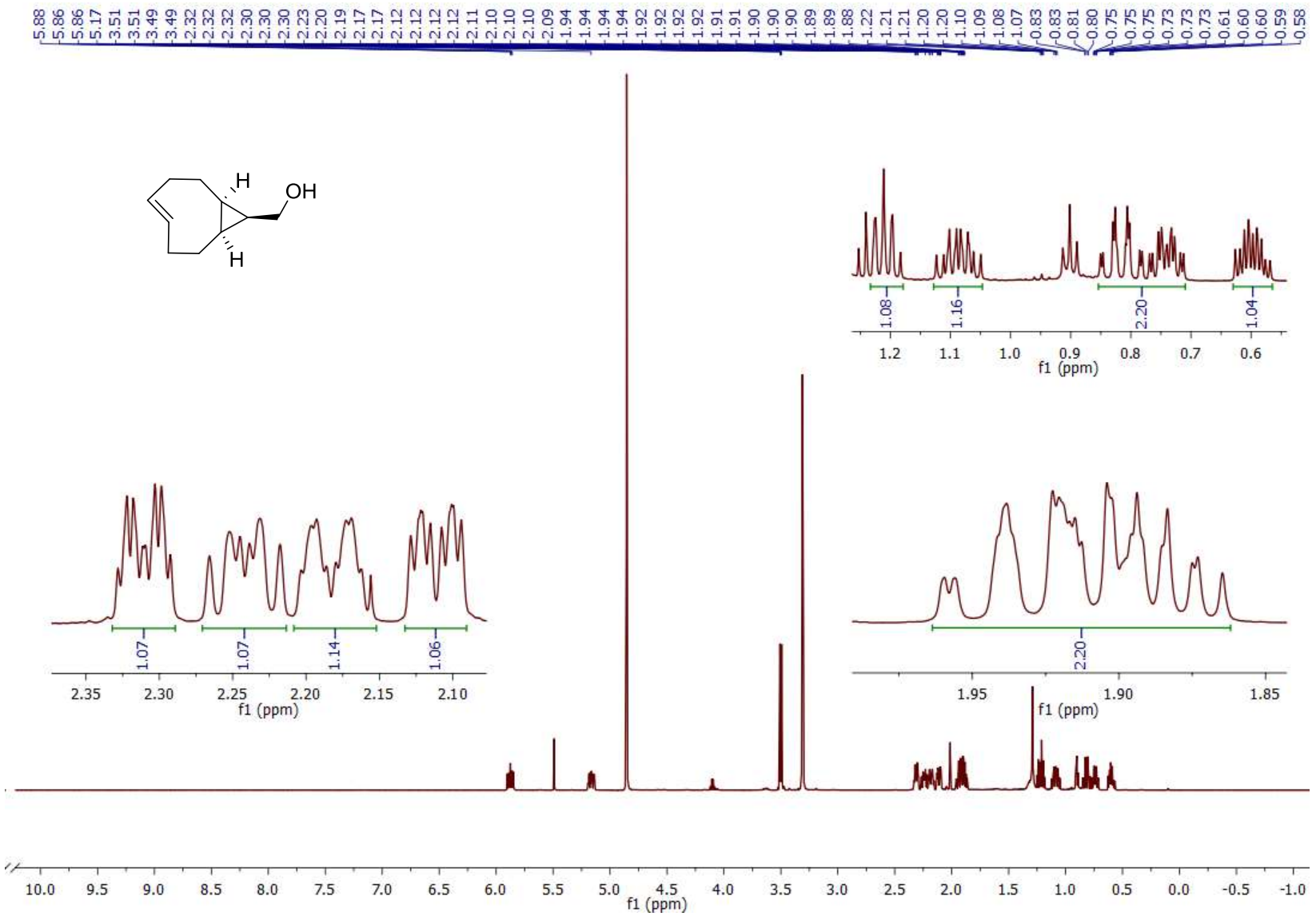

(rel-1R,8S,9S,4E)-Bicyclo[6.1.0]non-4-ene-9-ylmethanol (**2**)
^{1}H NMR (600 MHz, CD_3OD)

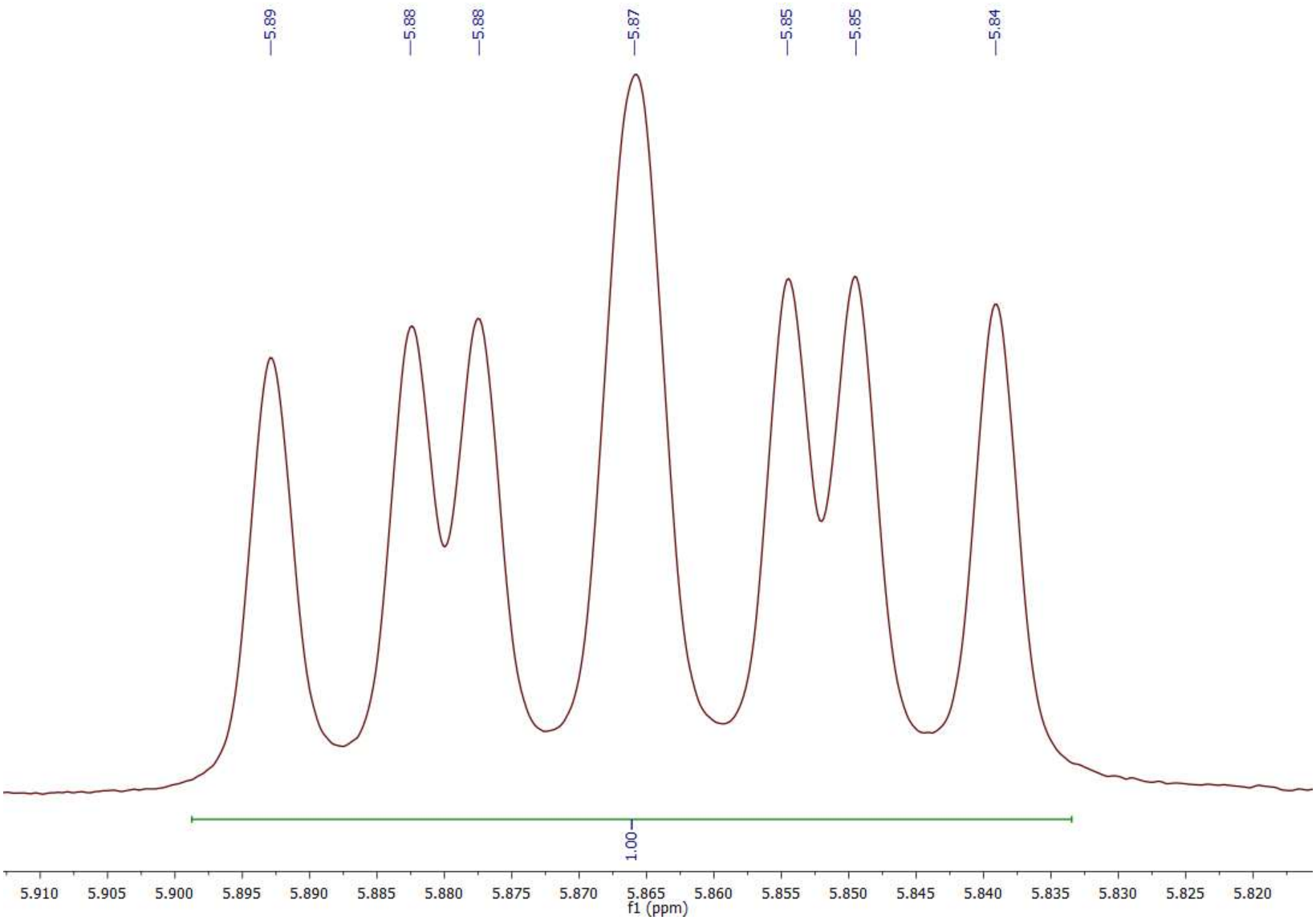

(rel-1R,8S,9S,4E)-Bicyclo[6.1.0]non-4-ene-9-ylmethanol (**2**)
^{1}H NMR (600 MHz, CD_3OD)

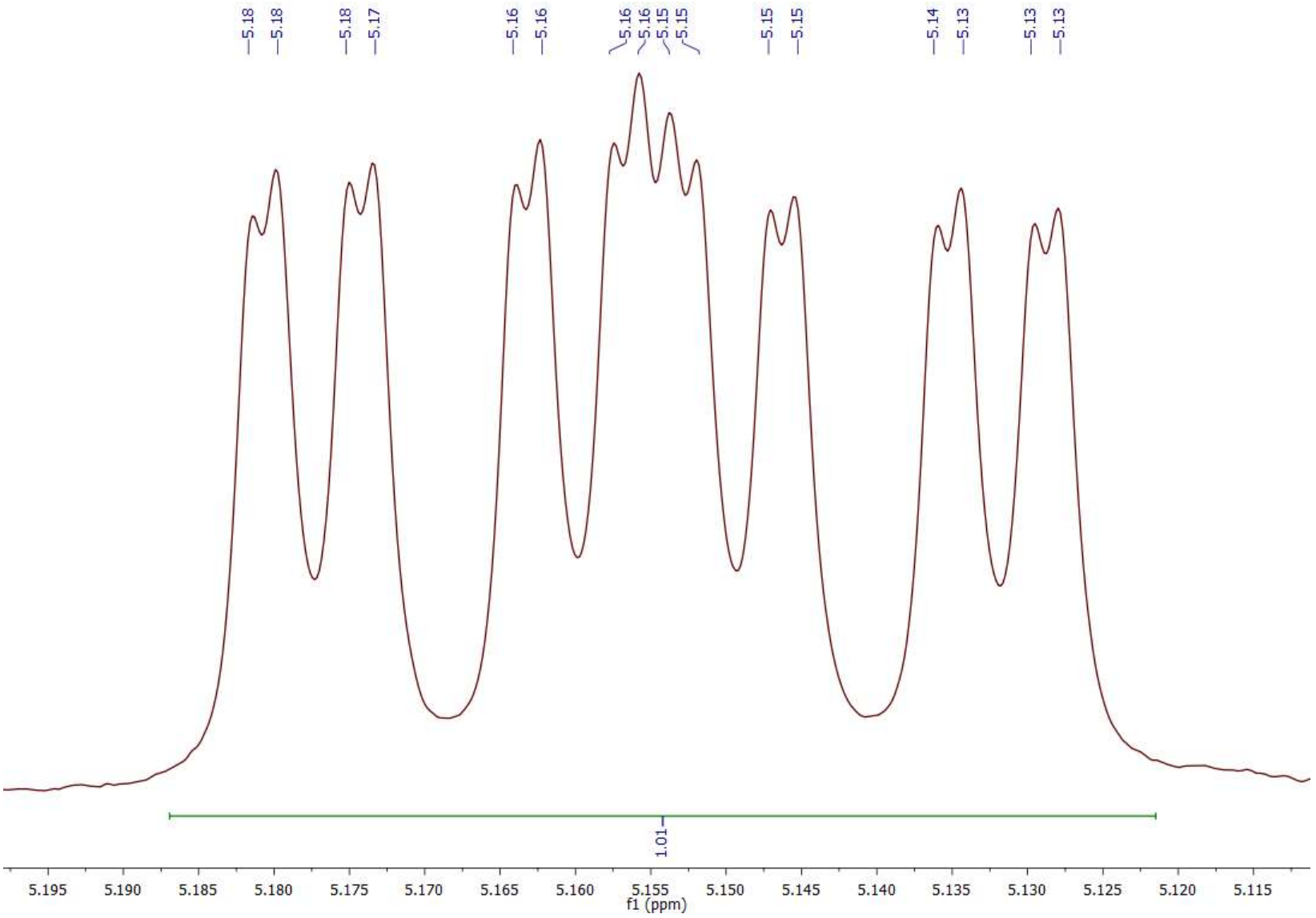

(rel-1R,8S,9S,4E)-Bicyclo[6.1.0]non-4-ene-9-ylmethanol (**2**)
^{1}H NMR (600 MHz, CD_3OD)

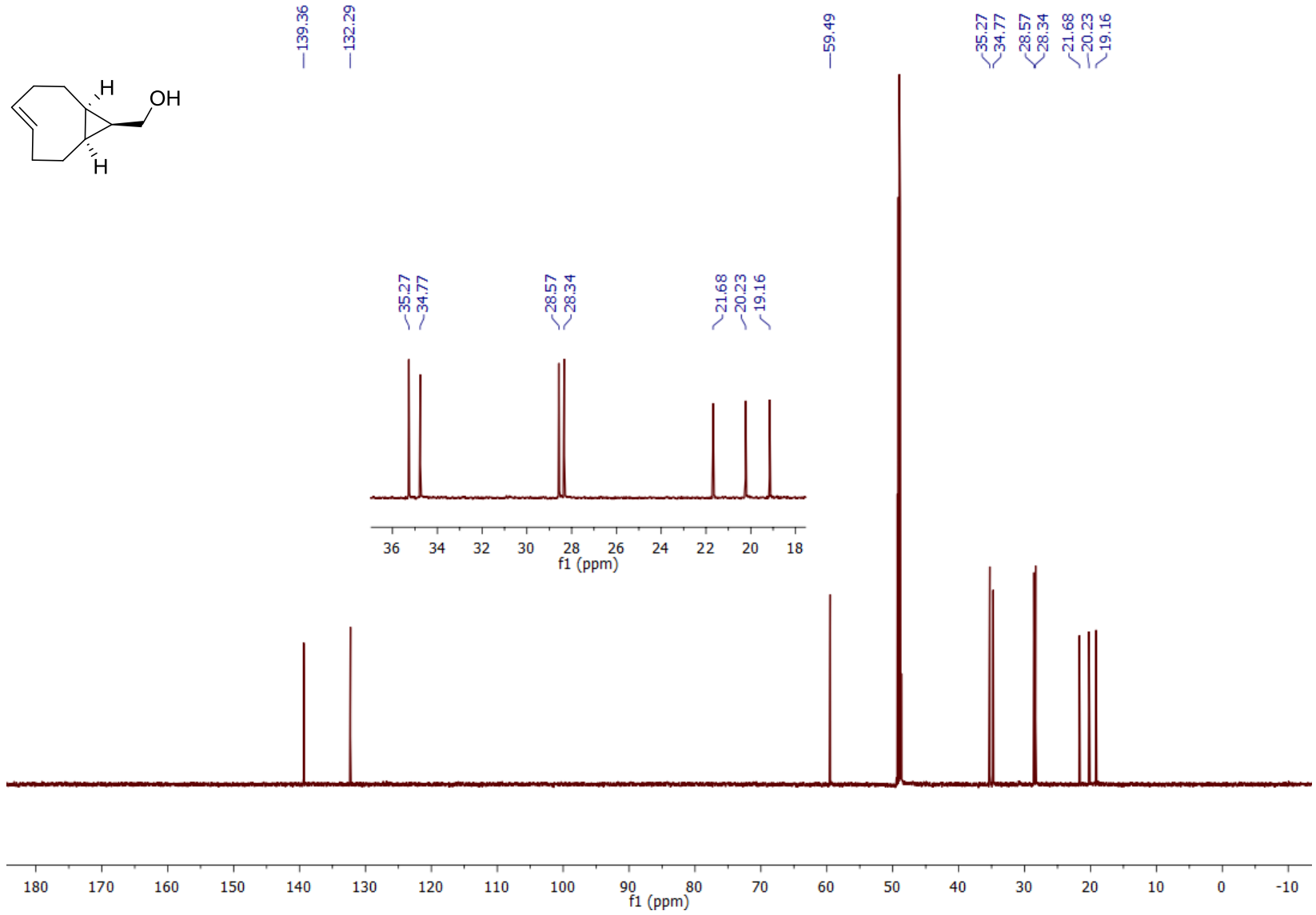

2-(2-(2-((*syn*-(*E*)-bicyclo[6.1.0]non-4-en-9-yl)methoxy)ethoxy)ethoxy)ethyl 4-methylbenzenesulfonate (**3**)
^{1}H NMR (600 MHz, CD_3OD)

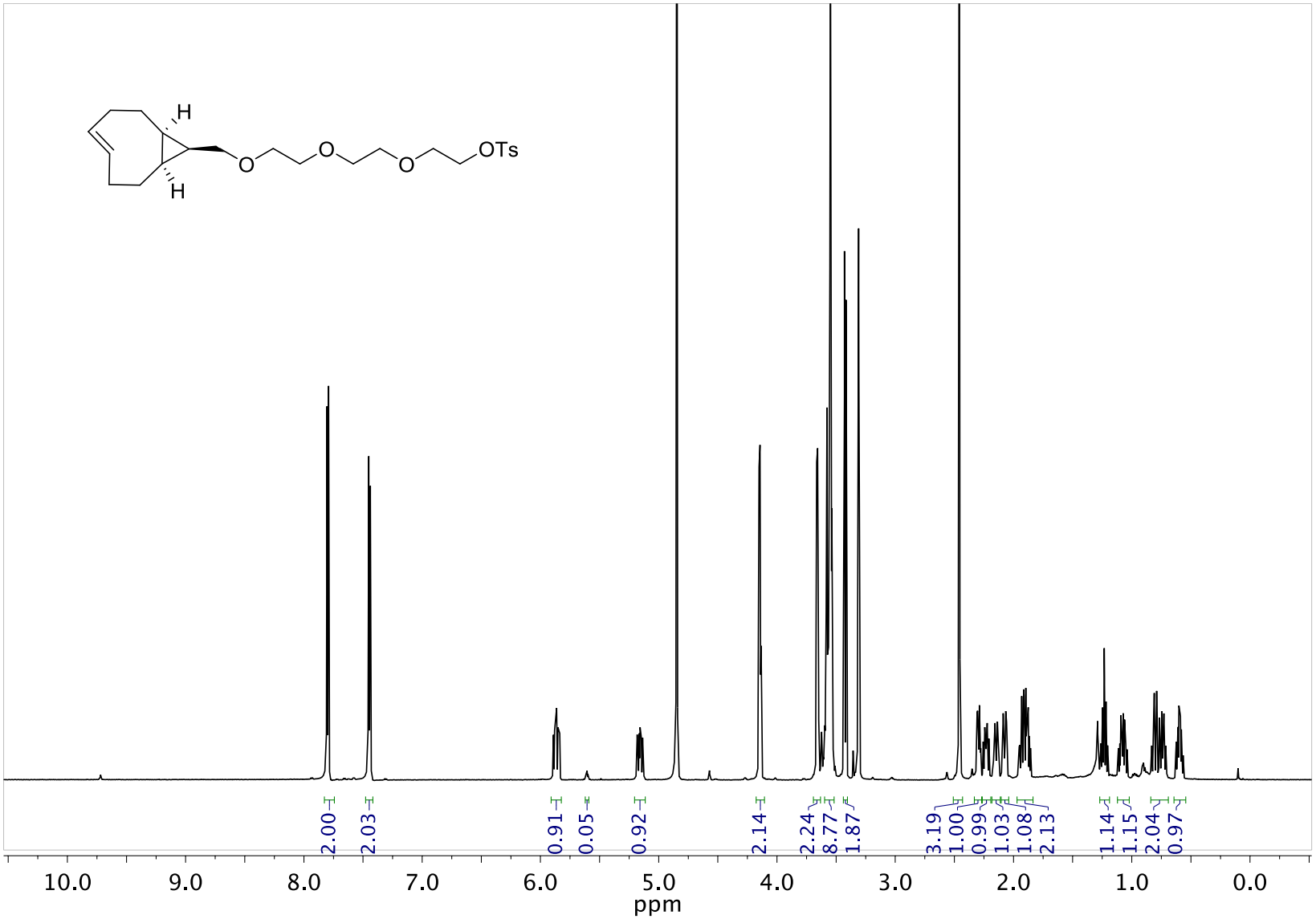

2-(2-(2-((*syn*-(*E*)-bicyclo[6.1.0]non-4-en-9-yl)methoxy)ethoxy)ethoxy)ethyl 4-methylbenzenesulfonate (**3**)
^{1}H NMR (400 MHz, CD_3OD)

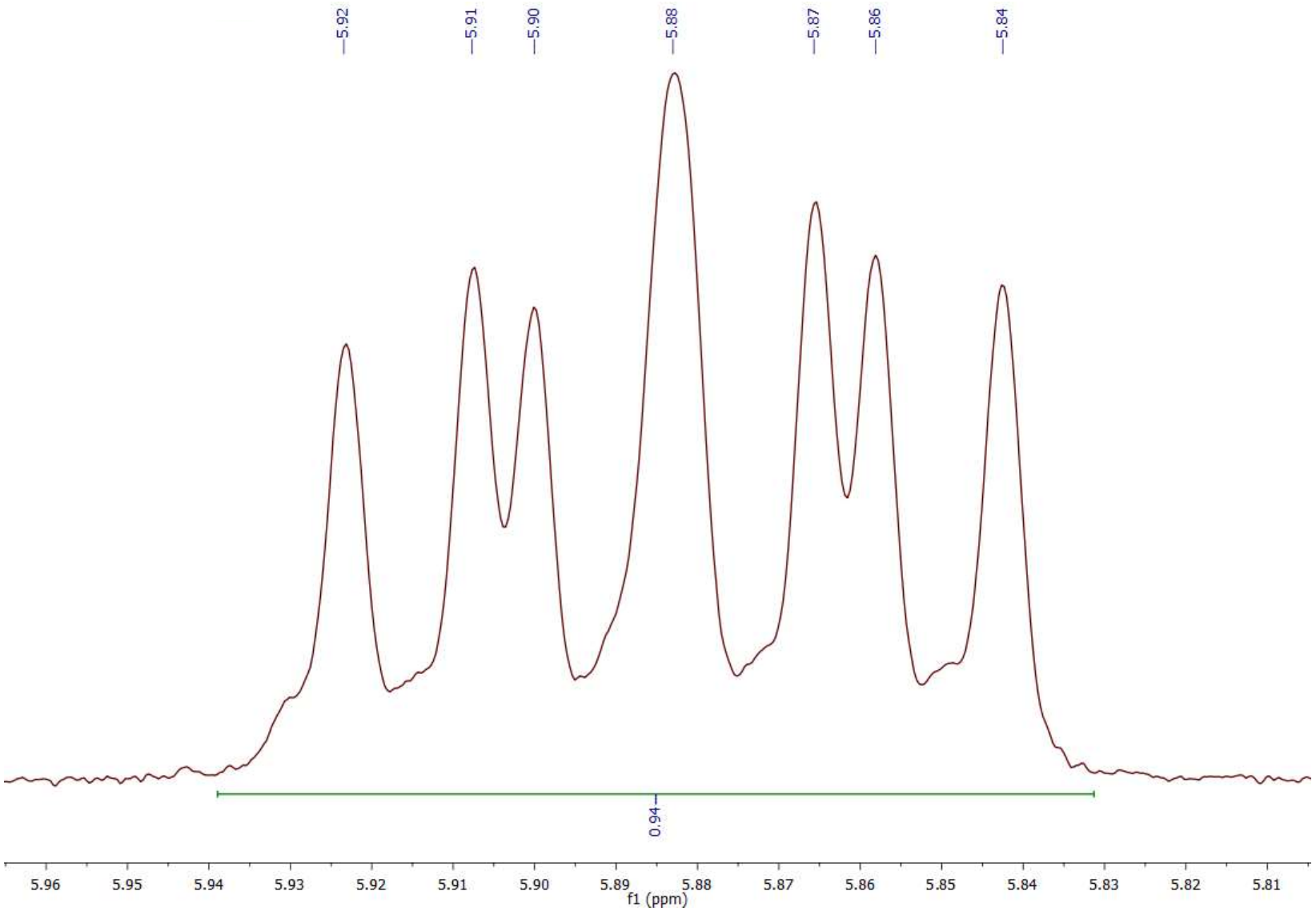

2-(2-(2-((*syn*-(*E*)-bicyclo[6.1.0]non-4-en-9-yl)methoxy)ethoxy)ethoxy)ethyl 4-methylbenzenesulfonate (**3**)
^{1}H NMR (400 MHz, CD_3OD)

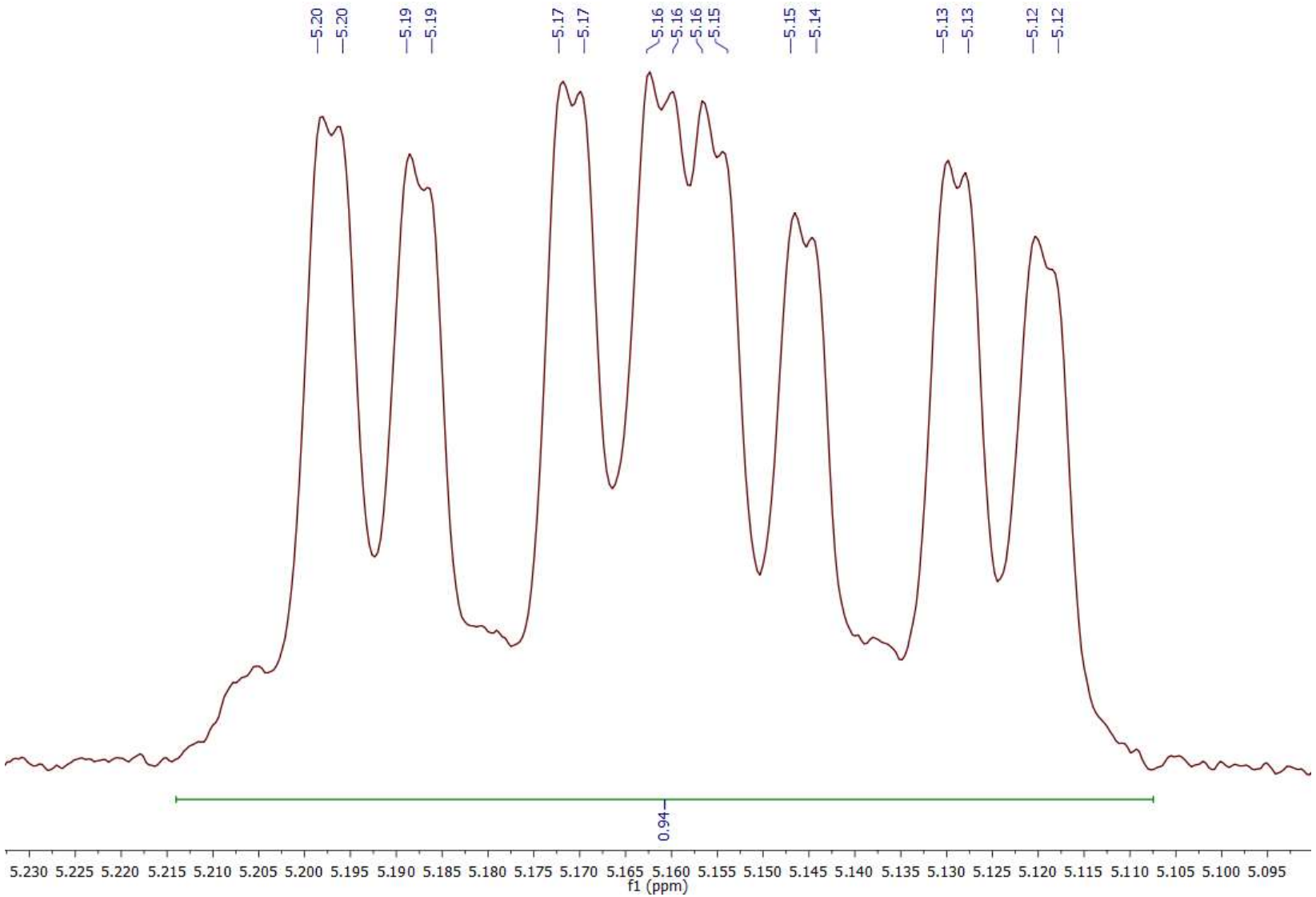

2-(2-(2-((*syn*-(*E*)-bicyclo[6.1.0]non-4-en-9-yl)methoxy)ethoxy)ethoxy)ethyl 4-methylbenzenesulfonate (**3**)
^{13}C APT NMR (100.6 MHz, CD_3OD)

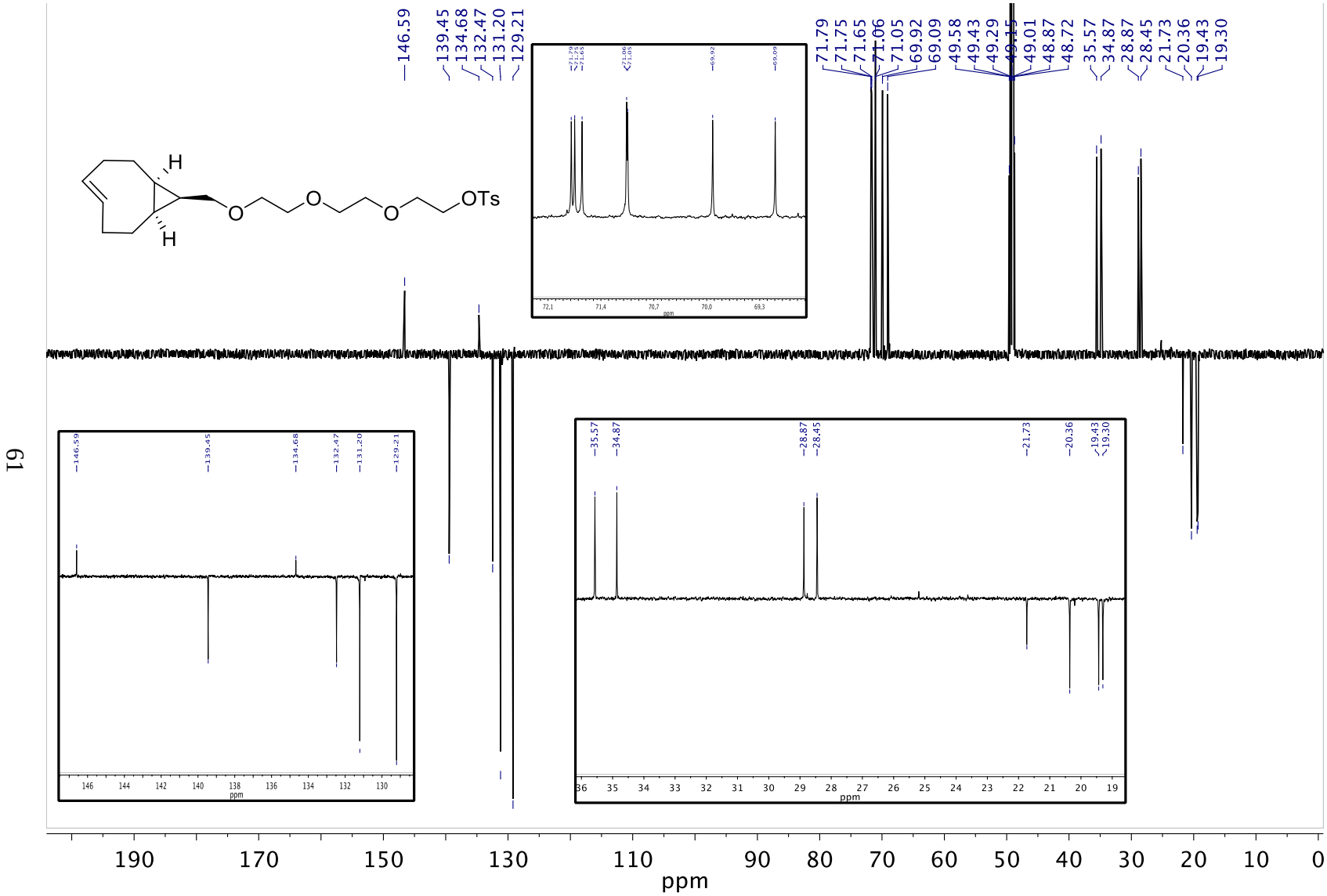

syn-(*E*)-9-((2-(2-(2-fluoroethoxy)ethoxy)ethoxy)methyl)bicyclo[6.1.0]non-4-ene (**^{18}F-4**)

^{1}H NMR (600 MHz, CD_3OD)

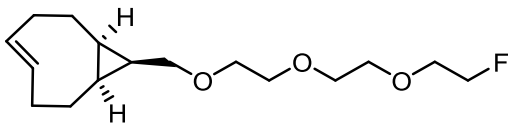

***Cis Isomer**

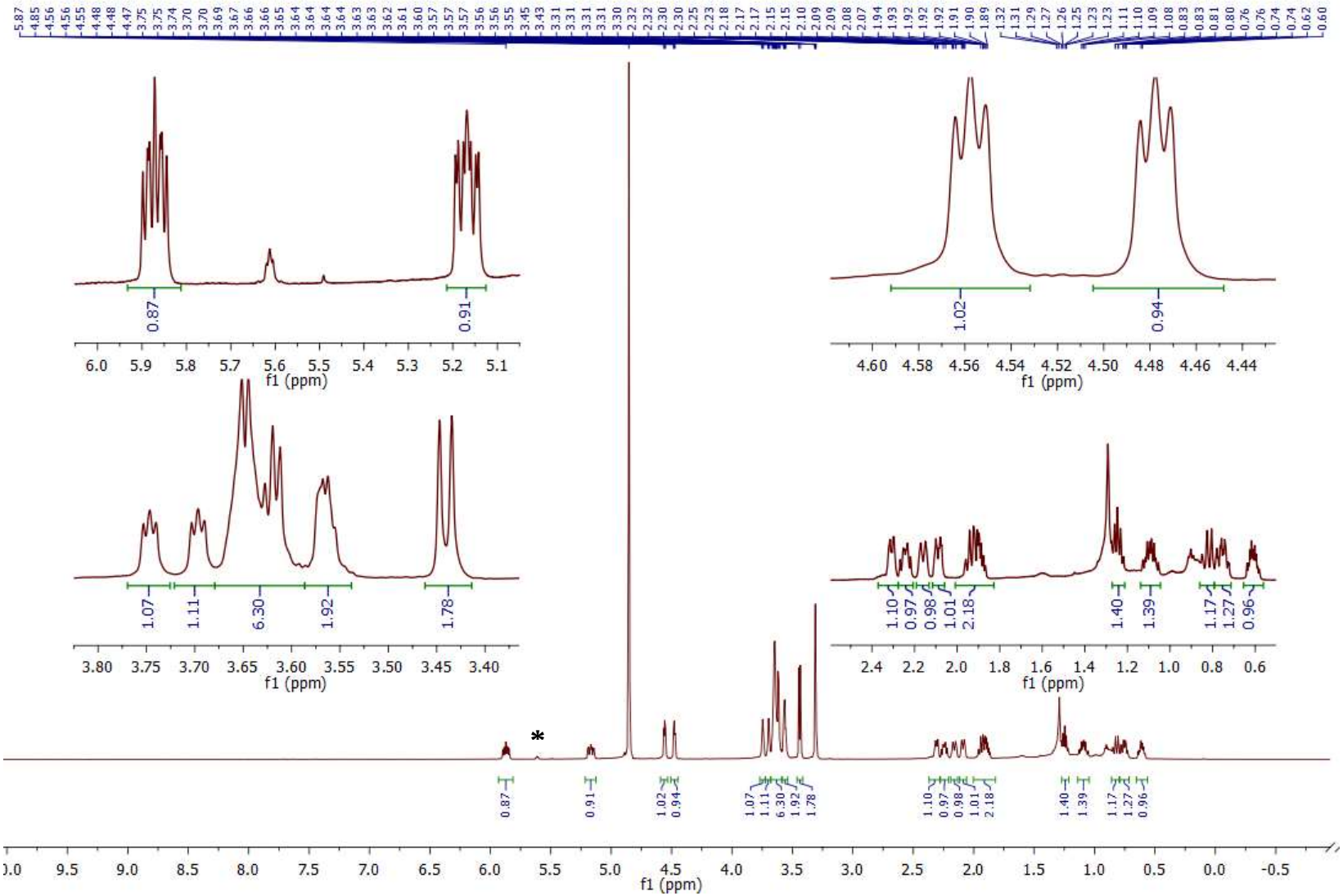

syn-(*E*)-9-((2-(2-(2-fluoroethoxy)ethoxy)ethoxy)methyl)bicyclo[6.1.0]non-4-ene (**^{18}F-4**)

^{13}C APT NMR (100.6 MHz, CD_3OD)

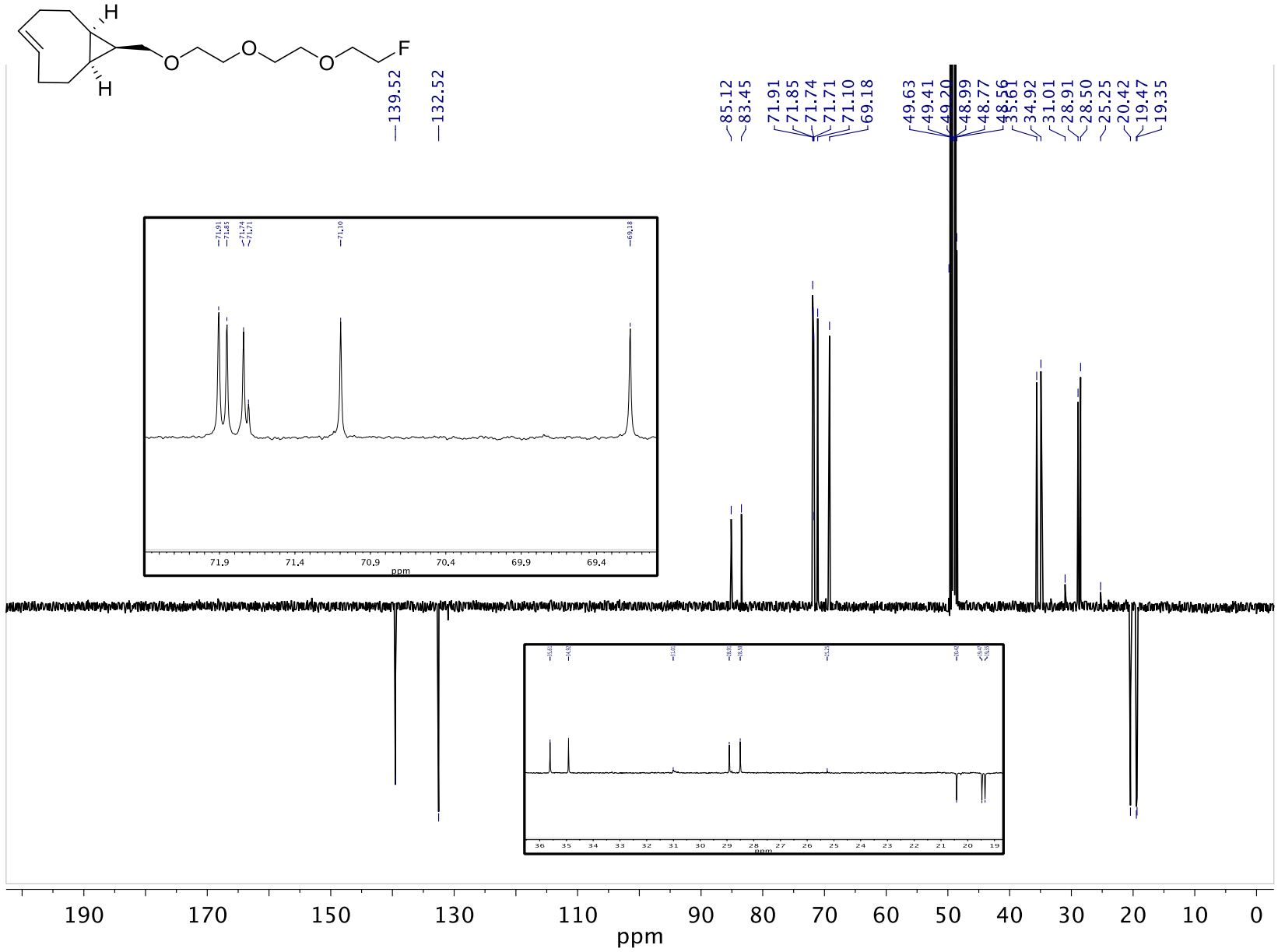

syn-(*E*)-9-((2-(2-(2-fluoroethoxy)ethoxy)ethoxy)methyl)bicyclo[6.1.0]non-4-ene (**^{18}F-4**)
^{19}F NMR (376 MHz, CD_3OD)

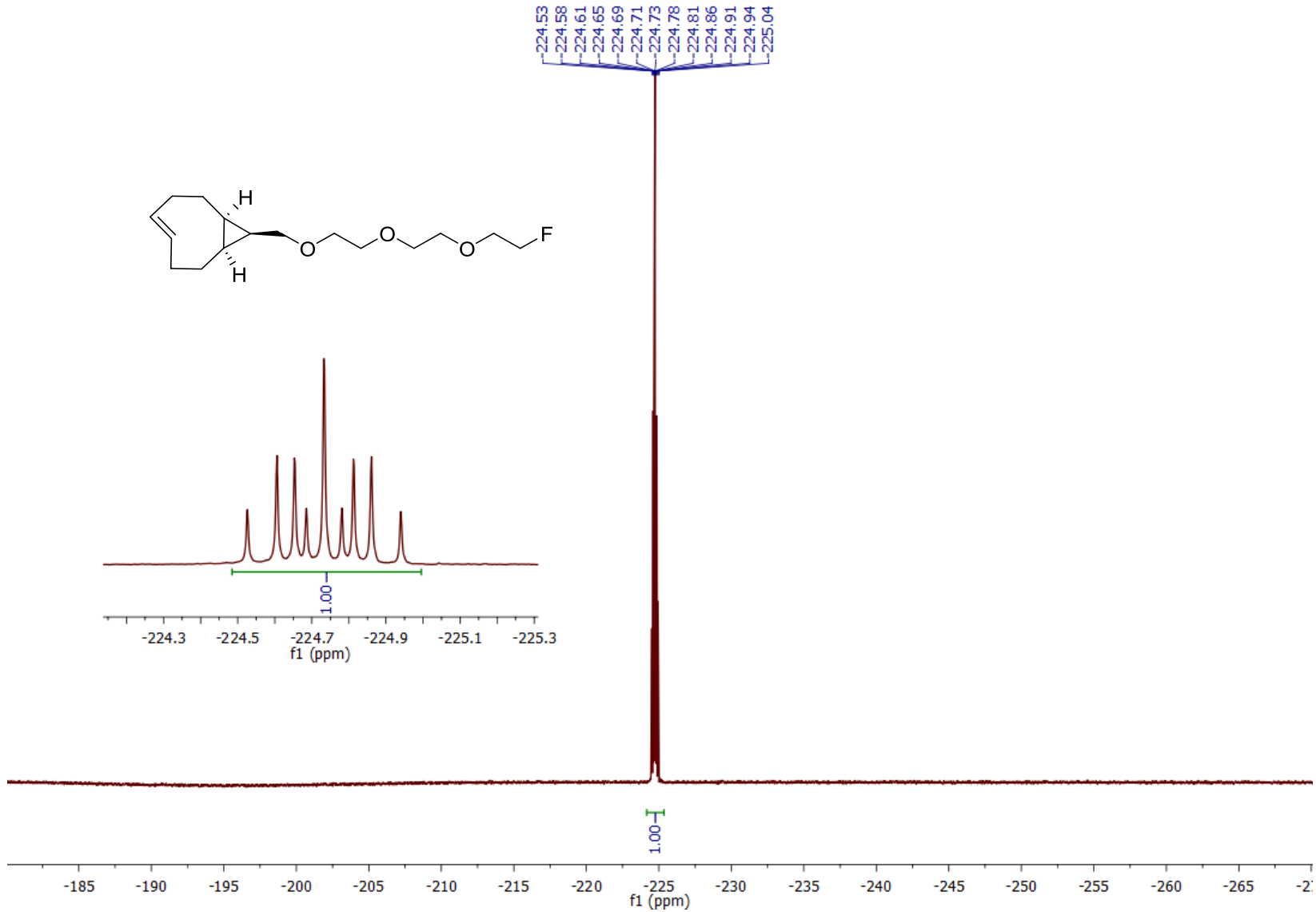

3-oxo-1-(4-(6-phenyl-1,2,4,5-tetrazin-3-yl)phenyl)-2,7,10,13,16,19,22,25,28,31,34,37,40-tridecaoxa-4-azatritetracontan-43-oic acid (**6**)
^{1}H NMR (400 MHz, CD_2Cl_2)

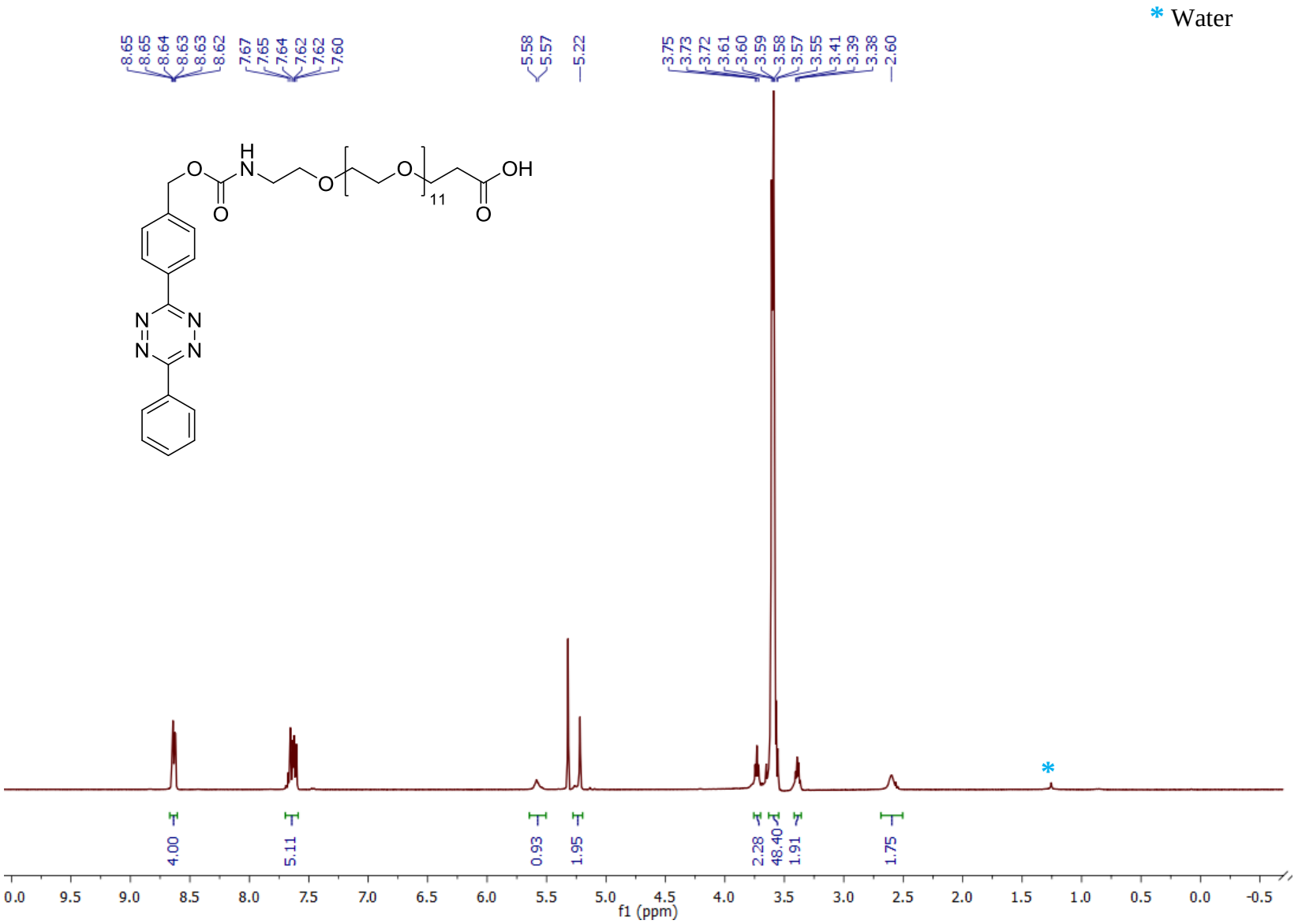

3-oxo-1-(4-(6-phenyl-1,2,4,5-tetrazin-3-yl)phenyl)-2,7,10,13,16,19,22,25,28,31,34,37,40-tridecaoxa-4-azatritetracontan-43-oic acid (**6**)

^{13}C NMR (101 MHz, $CDCl_3$)

*Dichloromethane

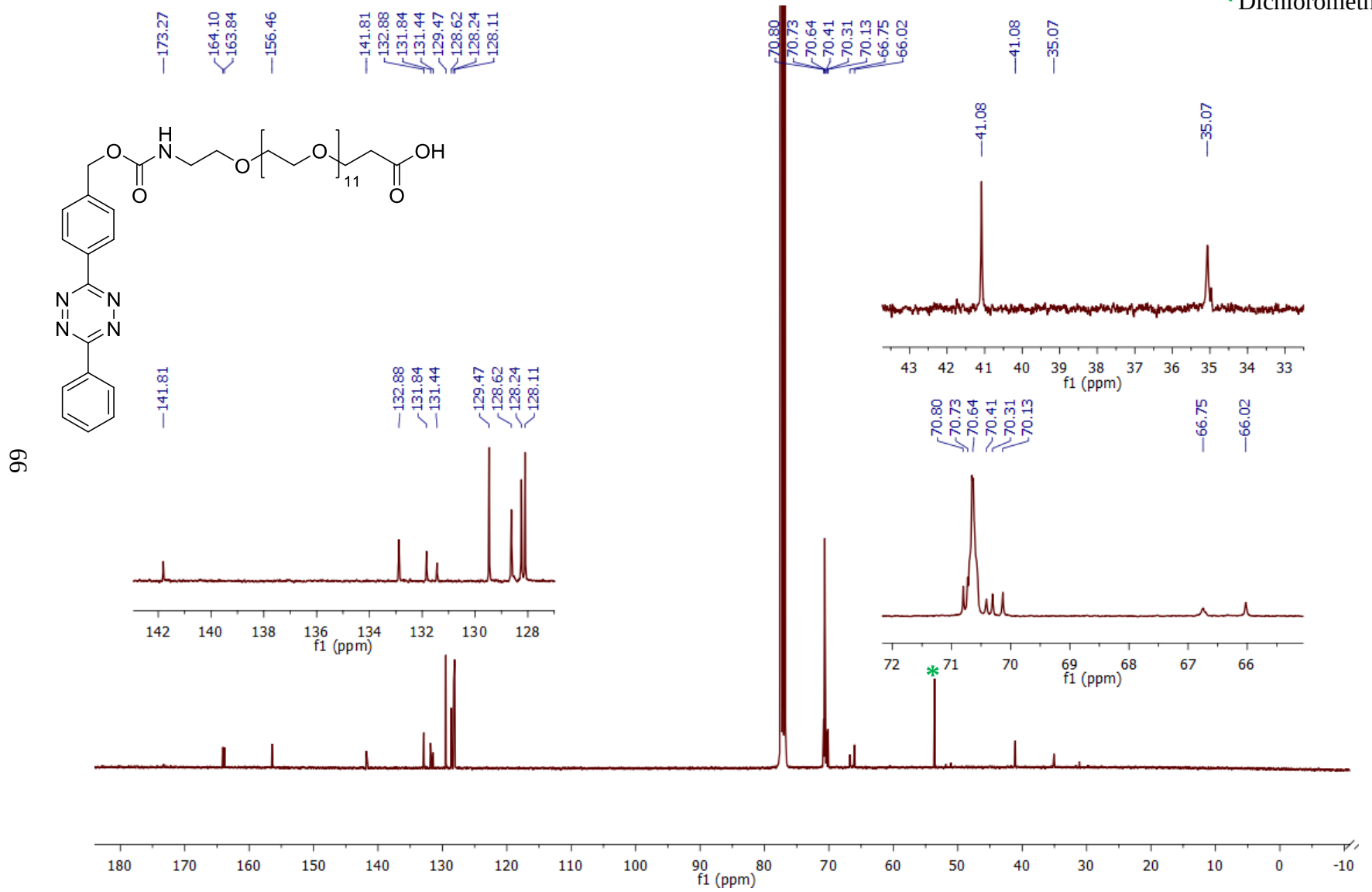

2,5-dioxopyrrolidin-1-yl 3-oxo-1-(4-(6-phenyl-1,2,4,5-tetrazin-3-yl)phenyl)-2,7,10,13,16,19,22,25,28,31,34,37,40-tridecaoxa-4-azatritetracontan-43-oate (**6a**)

^{1}H NMR (400 MHz, CD_2Cl_2)

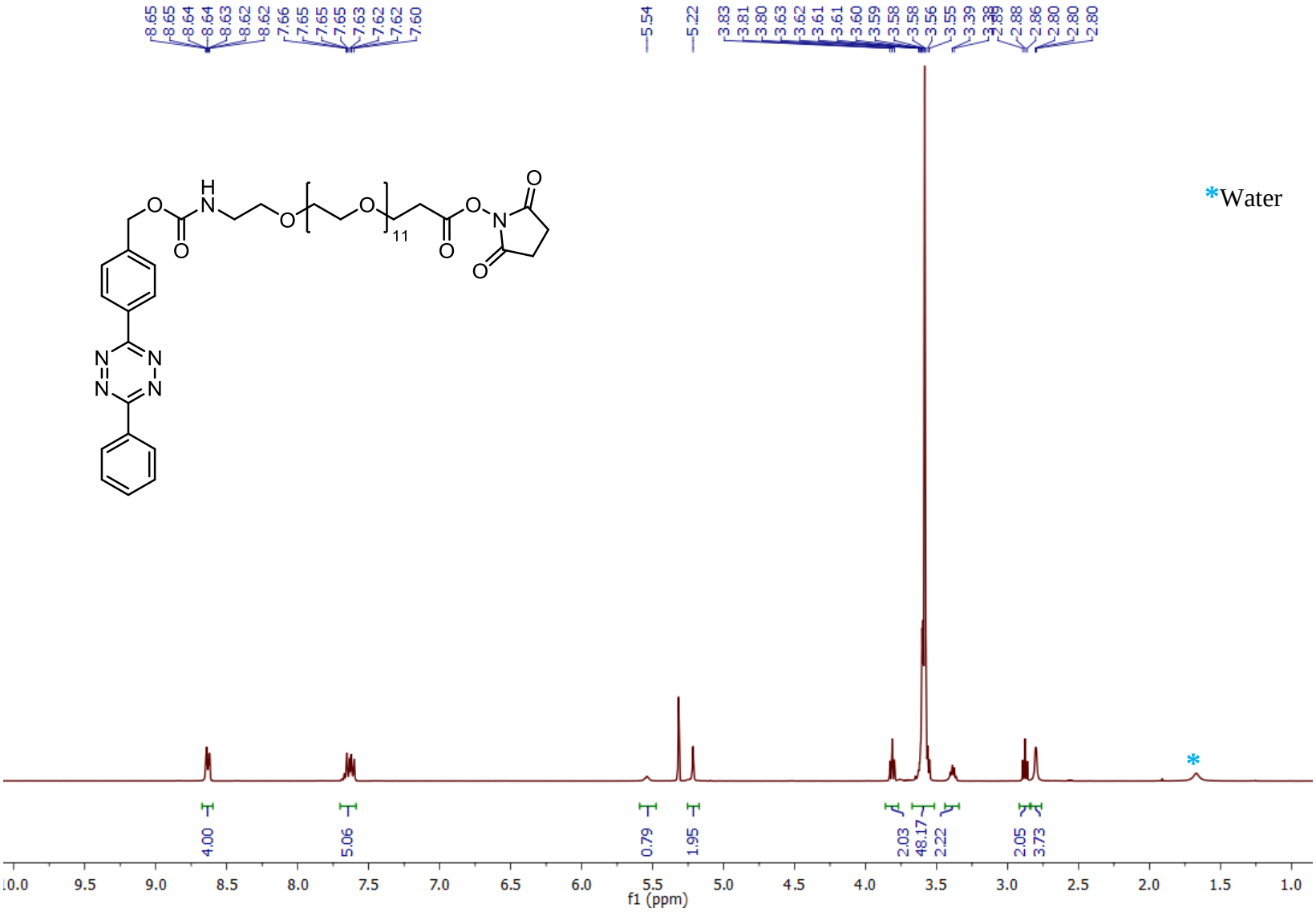

2,5-dioxopyrrolidin-1-yl 3-oxo-1-(4-(6-phenyl-1,2,4,5-tetrazin-3-yl)phenyl)-2,7,10,13,16,19,22,25,28,31,34,37,40-tridecaoxa-4-azatritetracontan-43-oate (**6a**)

^{13}C NMR (101 MHz, CD_2Cl_2)

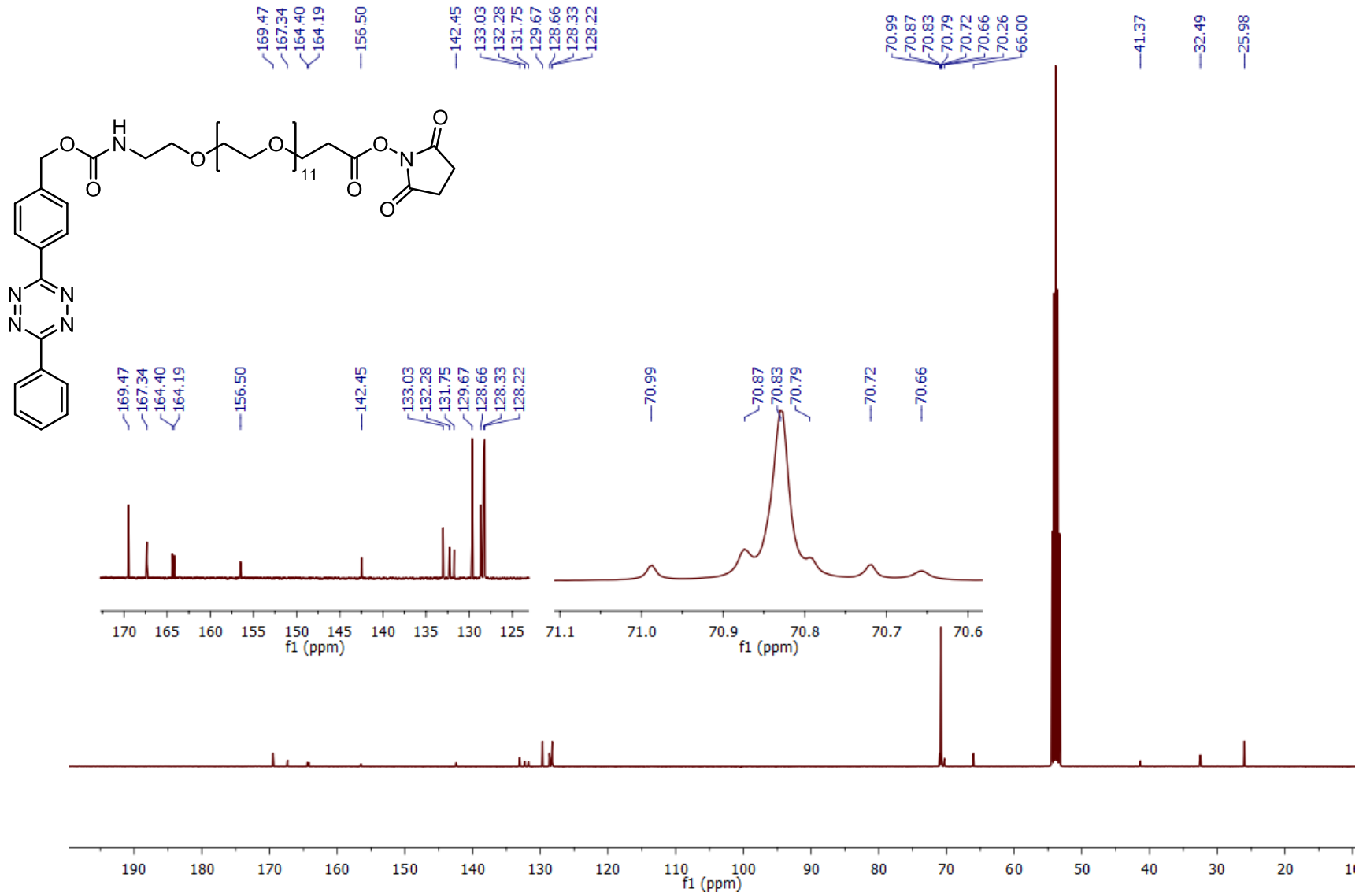

Appendix B

ADDITIONAL EXPERIMENTAL DATA FOR CHAPTER 1

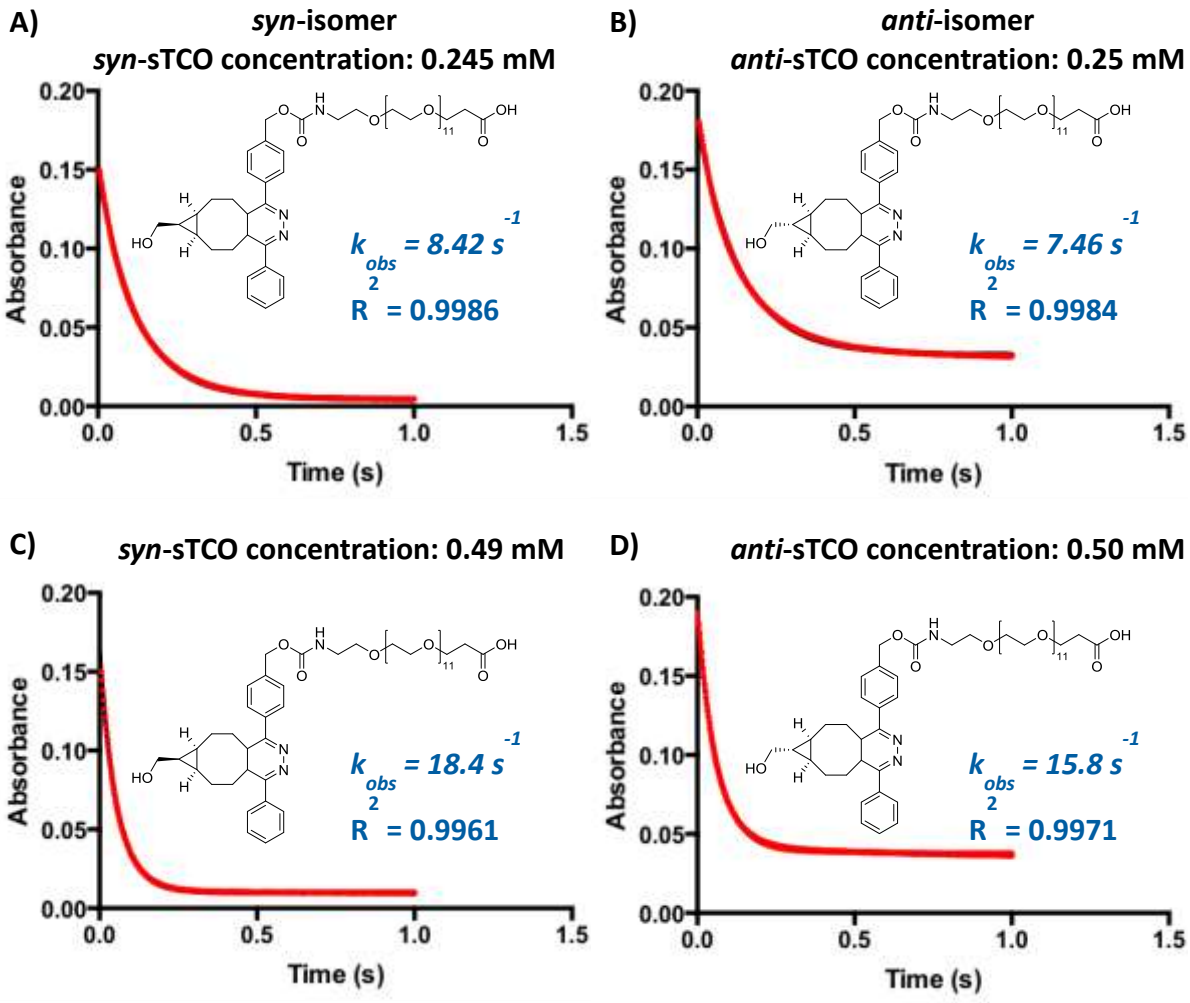

Figure A1: Stopped-flow monitored reaction of **6** (0.05mM) with ***syn*** and ***anti***-diastereomers of sTCO. Each plot represents the average of 4 kinetic runs. The concentration of the sTCO used in each kinetic data set is given about in each plot.

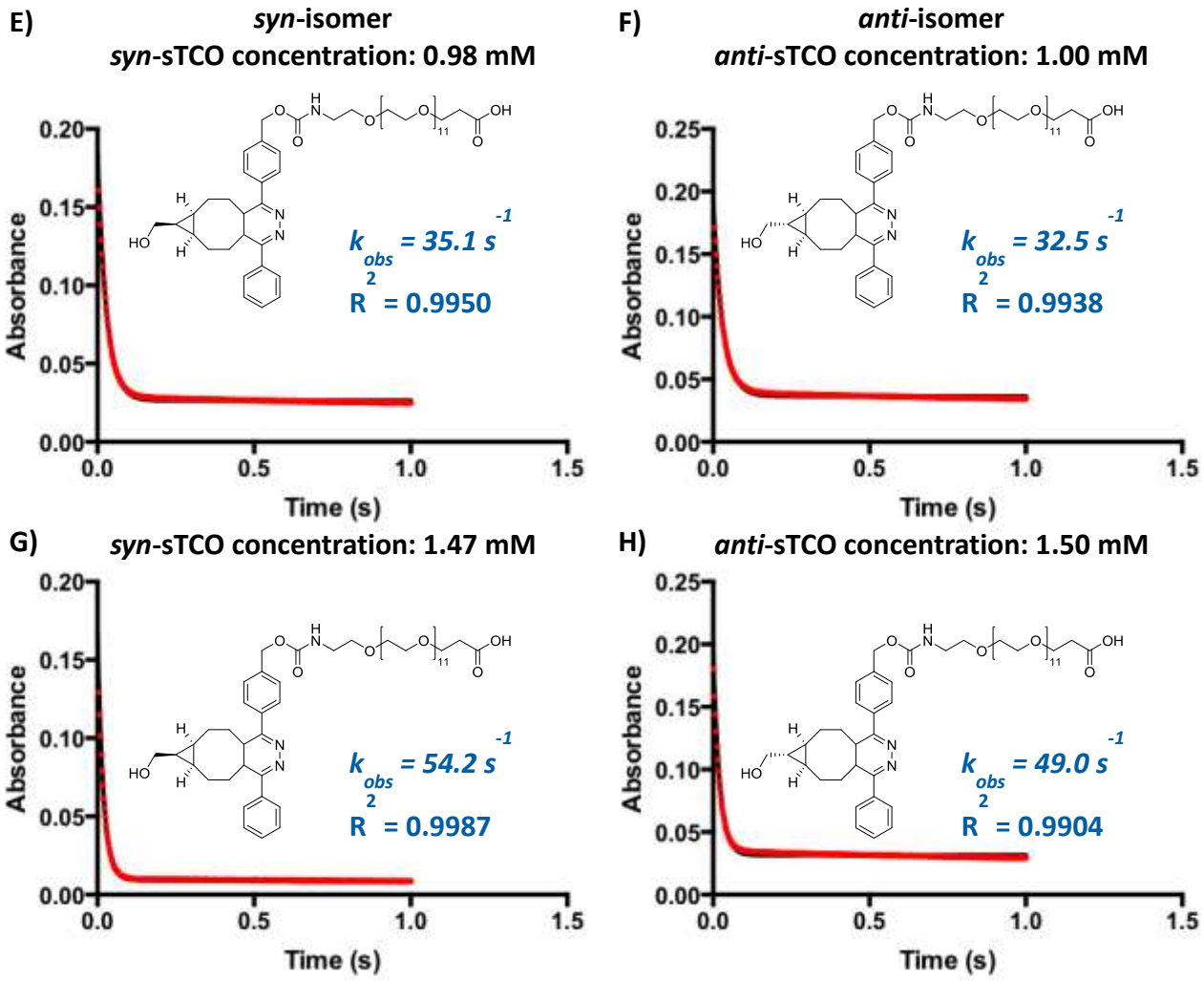

Figure A1 (continued): Stopped-flow monitored reaction of **6** (0.05mM) with ***syn*** and ***anti***-diastereomers of sTCO. Each plot represents the average of 4 kinetic runs. The concentration of the sTCO used in each kinetic data set is given about in each plot.

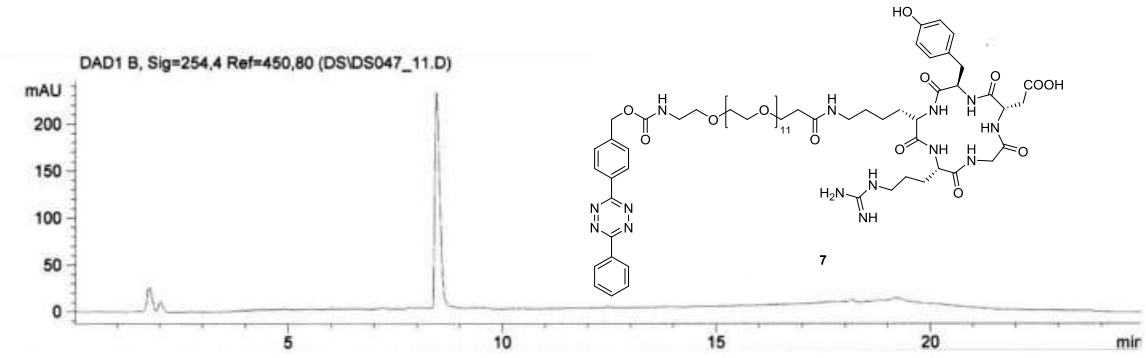

Figure A2: Reverse phase HPLC of purified **7**. Conditions: C18 Halo-column, 3.0 x 0.75 mm, 2.7 µM. HPLC solvents were modified by 0.1% formic acid. The chromatograph was carried out with a gradient from 10% water in acetonitrile at t = 0 min., to 100% acetonitrile at t = 10 min., which was then held until the end of the run at t = 20 min.

Appendix C

SPECTRAL DATA FOR CHAPTER 3

2-(2-(2-((*syn*-(*E*)-bicyclo[6.1.0]non-4-en-9-yl)methoxy)ethoxy)ethoxy)ethyl 4-methylbenzenesulfonate-AgNO3 (**14**)
^{1}H NMR (600 MHz, MeOD)

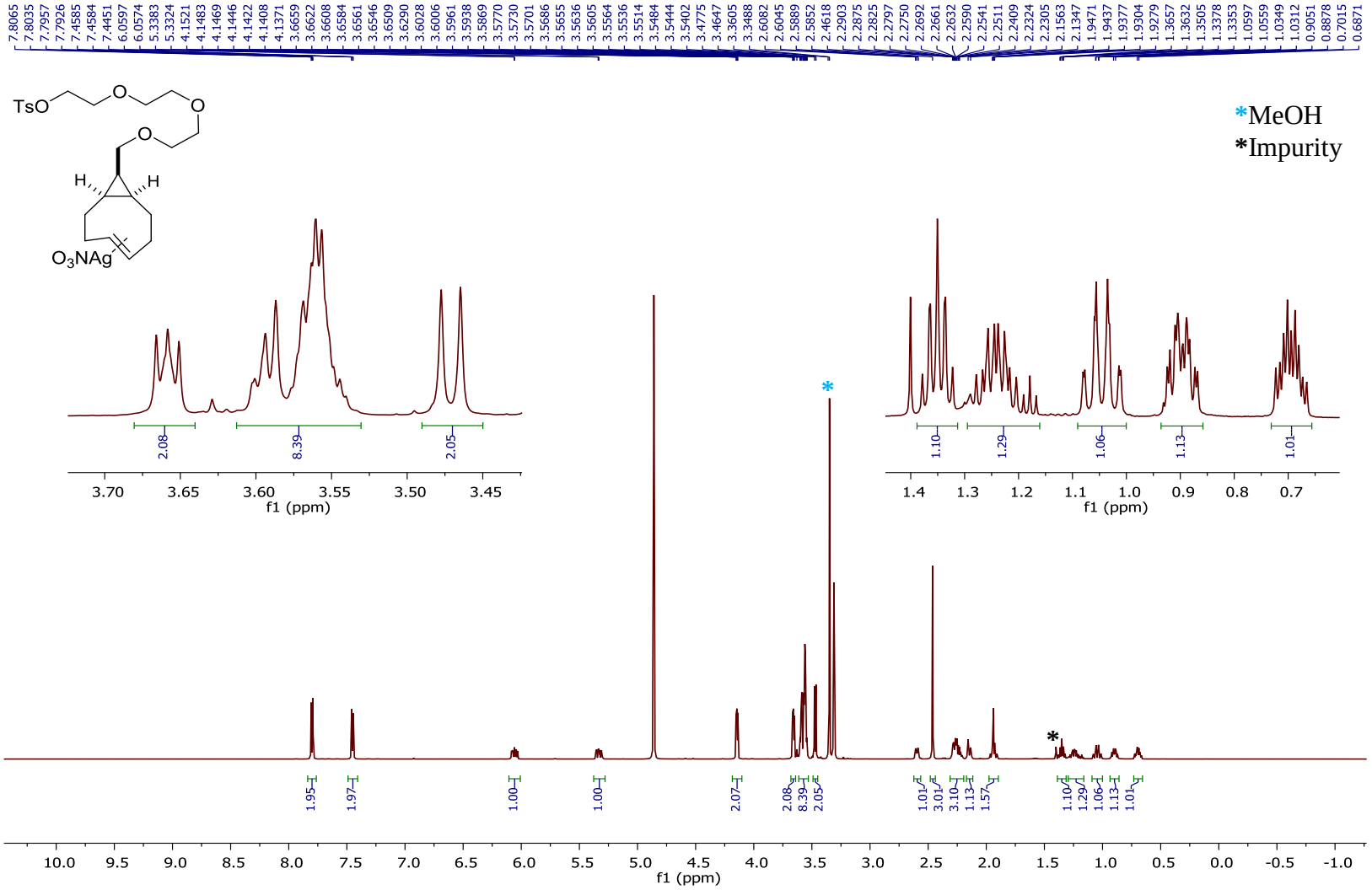

2-(2-(2-((*syn*-(*E*)-bicyclo[6.1.0]non-4-en-9-yl)methoxy)ethoxy)ethoxy)ethyl 4-methylbenzenesulfonate-AgNO3 (**14**)

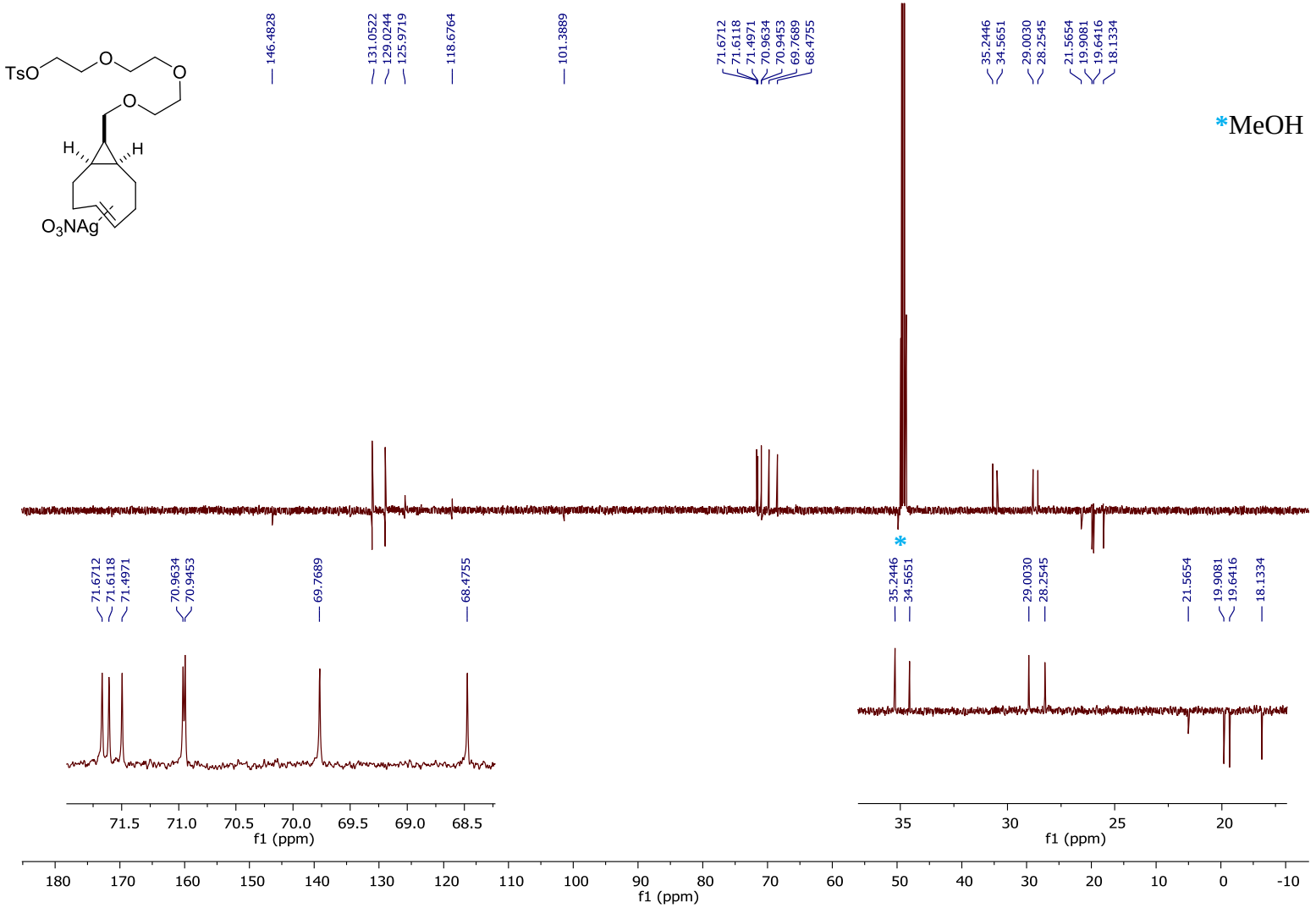

Appendix D

PERMISSION TO REPRINT MATERIALS IN CHAPTER 1

RE: [THNO Inquiry] permission for reprint Inbox x

Theranostics Publishing Team <publish@thno.org> Nov 29 (6 days ago)

to me

Thanks for your email. As an author or co-author of the article, you are free to include or reuse the materials in other articles or thesis or other publications that you write, with citation of the original source. Permission is automatically granted.

Kind regards,
Publishing Team
Theranostics
http://www.thno.org

-----Original Message-----
From: Theranostics [mailto:publish@thno.org]
Sent: Saturday, November 19, 2016 1:56 AM
To: publish@thno.org
Subject: [THNO Inquiry] permission for reprint

To whom it may concern:
During this past year, I was a co-author on a paper published in Theranostics. With your permission, would it be acceptable to reprint some of this data for my Master's thesis?

Theranostics 2016; 6, 887-895. doi:10.7150/thno.14742

Thank you,
Katarina

Sender record
Name: Katarina Rohlfing
Sender Email: rohlfing@udel.edu
Sender Host: 128.4.103.21
Sender Institution: University of Delaware